Applications of Vibration-Based Occupant Inference in Frailty Diagnosis through Passive, In-Situ Gait Monitoring

Rafael dos Santos Gonçalves

Thesis submitted to the Faculty of the

Virginia Polytechnic Institute and State University

in partial fulfillment of the requirements for the degree of

Master of Science

in

Mechanical Engineering

Rodrigo Sarlo, Chair

Oumar Barry

Robert L. West

August 10, 2021

Blacksburg, Virginia

Keywords: Frailty, Gait Analysis, Footstep Localization, Accelerometers, Smart Buildings

Applications of Vibration-Based Occupant Inference in Frailty Diagnosis through Passive, In-Situ Gait Monitoring

Rafael dos Santos Gonçalves

(ABSTRACT)

This work demonstrates an application of Vibration-Based Occupant Inference (VBOI) in frailty analysis. The rise of both Internet-of-Things (IoT) and VBOI provide new techniques to perform gait analysis via footstep-induced vibration which can be analyzed for early detection of human frailty. Thus, this work provides an application of VBOI to passively track gait parameters (e.g., gait speed) using floor-mounted accelerometers as opposed to using a manual chronometer as it is commonly performed by healthcare professionals.

The first part of this thesis describes the techniques used for footstep detection by measuring the power of the footstep-generated vibration waves. The extraction of temporal gait parameters from consecutive footsteps can then be used to estimate temporal features such as cadence and stride time variation.

VBOI provides many algorithms to accurately detect when a human-induced vibration event happened, however, spatial information is also needed for many gait parameters used in frailty diagnosis. Detecting where an event happened is a complicated problem because footsteps waves travel and decay in different ways according to the medium (floor system), the number of people walking, and even the walking speed. Therefore, the second part of this work will utilize an energy-based approach of footstep localization in which it is assumed that footstep waves decay exponentially as they travel across the medium. The results from this approach are then used to calculate spatial and tempo-spatial parameters.

The main goal of this study is to understand the applicability of VBOI algorithms in gait analysis for frailty detection in a healthcare setting.

Applications of Vibration-Based Occupant Inference in Frailty Diagnosis through Passive, In-Situ Gait Monitoring

Rafael dos Santos Gonçalves

(GENERAL AUDIENCE ABSTRACT)

Human frailty is responsible for one of the highest healthcare costs and the death of many people every year. Although anyone suffering from frailty has a higher chance of death, it is particularly dangerous for the elderly population and for those suffering from other comorbidities. Diagnosing frailty is hard because it usually happens slowly over time. However, it has been shown that changes in some walking parameters (such as gait speed) can be an early indication of frailty. Many technologies have been created in order to track gait parameters, many of which either require expensive equipment (e.g., force plates) or the use of wearable devices, which can introduce privacy concerns.

It has been proposed in the literature that Vibration-Based Occupant Inference (VBOI) techniques could be used in healthcare applications. Such algorithms measure footstep-induced vibration waves in order to detect and track footsteps. This system can provide several advantages in frailty analysis because of its affordability, ease of use, and little impact on patients' privacy. Therefore, the aim of this study is to understand the applicability of VBOI algorithms in gait analysis for frailty detection to be used in a healthcare setting. This thesis will proceed as follows:

- First, the demonstration of an energy-based footstep detection and localization algorithm in VBOI.

- Second, the application of such algorithms for gait parameters extraction with simulated frail walkers.
- Finally, an analysis of the proposed VBOI techniques for deployment in a real hospital setting.

Dedication

To my mother, *Simone*...

to my grandfather, *Antônio Carneiro*...

to my great-grandmother, *Maria Pires*...

and to *Mauricio Calicchio*, *Lígia Calicchio*, and *Mauricio Jr.*

Acknowledgments

The author would like to thank the members of the Master's advisory committee for their support. In particular, the author is incredibly thankful to the committee head, Dr. Rodrigo Sarlo, for his essential help during the entire author's Master's journey, especially at major challenges in the research project.

The presented work was conducted in the Vibrations, Informatics, and Built Environments (VIBEs) Lab at Virginia Tech, and the author is grateful to his lab mates for their advice, feedback, and help during walking experiments.

The author is also thankful for the support and help received from collaborators Dr. Tiffany Drape, Dr. Robin Queen, and Dr. Joseph Scarpa, whose expertise and guidance were essential in understanding key frailty concepts and how they relate to gait.

Finally, the author is extremely thankful for the never-ending support and love received from the author's family and friends, without which this work would have not been possible.

Contents

List of Figures

List of Tables

List of Abbreviations

CHS Cardiovascular Health Study

CSHA Canadian Study of Health and Aging

CV Coefficient of Variation

FEEL Force Estimation and Event Localization

FGT Frail Gait Trials

GH Goodwin Hall

GPS Global Positioning System

HGT Healthy Gait Trials

HS Heel Strike

IMU Inertial Measurement Unit

IoT Internet-of-Things

MAE Mean Absolute Error

MD Mean Absolute Difference

RSS Received Signal Strength

SNR Signal-to-Noise Ratio

TDOA Time-Difference of Arrival

TO Toe off

TOA Time-of-Arrival

VBOI Vibration-Based Occupant Inference

Chapter 1

Introduction

Frailty is a health condition that is highly prevalent in the elderly community and is responsible for a significant increase in negative health outcomes such as falls, hospitalizations, and mortality [32]. The main characteristic of frailty is the loss of the physiological reserves in the body and a functioning decline [32, 47], however, diagnosing frailty is hard because it depends on changes in many life factors such as health history, physical activity levels, mental health, and even eating habits. Therefore, healthcare providers must constantly perform frailty tests on patients in order to acquire enough evidence for a frailty diagnosis. Different frailty criteria indexes were developed in the literature to detect frailty, among which the one given by the Cardiovascular Health Study (CHS), also known as Fried's criteria, is the most adopted [65]. Fried's criteria classify patients as "frail" according to five factors: slow gait speed, low physical activity, intentional weight loss, exhaustion, and muscle weakness. However, many studies have shown that changes in gait speed are one of the strongest predictors of frailty [29, 32, 41, 66]. That is because walking is a complex event that involves coordinated work from multiple systems in the body such as the nervous, skeletal, and muscular ones. Thus, changes in gait speed can be indicative of an underlying health condition.

One of the current methods of measuring gait speed in healthcare involves taking time measurements with a stopwatch as a patient walks along a certain distance. This technique is not ideal because stopwatch measurements are susceptible to variability as they rely on the observer's judgment of when the patient completed the walk, and on the observer's

reaction time to take time measurements as accurately as possible. Tracking gait speed with a stopwatch also has the problem that only one parameter (gait speed) can be easily tracked, and although gait speed is an important frailty index, other gait parameters (such as cadence and stride time variability) can also provide further evidence of a frailty status.

Multiple new technologies have been developed recently with the rise of smart structures and internet-of-things (IoT). Particularly, vibration-based occupant inference (VBOI) has been used in a variety of applications for passively tracking building occupants walking along an instrumented floor system [11]. In fact, VBOI has been used before in building occupant gait analysis and has shown potential to be used in healthcare [38]. Therefore, the focus of this thesis will be on analyzing the performance and usability of VBOI techniques to gait analysis in frailty detection.

1.1 Motivation and Summary of Previous Gait Monitoring Methods in Frailty Detection

Multiple researchers have studied ways of tracking gait parameters in the literature for frailty analysis. These include using force plates/mats [24, 31, 45], motion capture devices [12, 41], and wearables [28].

The motivation for using VBOI techniques in frailty detection comes from the possible advantages of such algorithms when compared to others proposed in the literature. For example, video-based motion capture devices are among the most accurate ways to analyze gait [41], and they are able to track a large number of gait parameters. However, most of them work by the time-of-flight principle that usually requires the user to wear reflective devices at specific body locations for increased tracking accuracy. In addition, image-based

devices require a direct line-of-sight to the patient, which means that multiple cameras may be needed during walking trials. The methods provided by VBOI do not require the user to wear any electronic tags and are independent of a direct line-of-sight to the target. Although most VBOI localization algorithms require multiple sensors [10], these are more affordable than most state-of-art motion capture devices. Also, if the researcher is only interested in temporal gait parameters, such as cadence, Kessler et al. [38] showed that only one sensor is capable of accurately doing so up to 50 feet away from the footstep impact location.

Another category of gait tracking devices for frailty analysis includes force mats/plates. These surfaces are capable of measuring the pressure produced by footsteps, which can be used to estimate other interesting gait parameters in addition to image-based devices such as footstep force distribution. Similar to VBOI approaches, force mats do not require the patients to wear any electronic devices during tracking but they do require the patient to step on its surface. Therefore, force mats must cover the entire walking path. With VBOI, on the other hand, patients do not need to step at specific spots to have their gait parameters analyzed. However, as shown in Chapter 3, VBOI localization algorithms work best when footsteps happen inside the convex-hull of the sensors.

Wearable technologies propose solutions to most limitations from force mats and motion capture systems. Wearables are more affordable and have grown in popularity with the rise in commercially available smartwatches and fitness trackers. These devices usually contain multiple health tracking sensors, including an inertial measurement unit (IMU) that can be used to perform gait analysis. Since wearables can be connected to the internet and the patient's mobile device, they can also be used to send and receive text messages and phone calls and to localize the user via the global positioning system (GPS). These capabilities raise privacy concerns as wearables can be used to track personal information from users such as home location, contacts, and personal media [67]. Furthermore, as their name suggests,

wearables are active trackers when it comes to gait monitoring as they rely on the user to remember to wear them in order to have their health features tracked. On the other hand, VBOI algorithms do not violate the patient's privacy as only vibration signals are captured by accelerometers. They also work independently of the patient's awareness, opening the possibility of fast and effective gait tracking.

In summary, an array of vibration sensors can provide a system to passively detect and track patients via their footstep-generated vibration waves. Such a system has the advantage of being non-intrusive and affordable when compared to force mats or video image processing. In addition, VBOI techniques do not require the user to carry any electronic tracking devices nor do they need a reserved space to be set up. These techniques have been well studied in occupant localization tracking [9, 10, 11, 21], energy conservation [48], and even in localizing an active shooter in a building [37]. Given the proposed benefits of VBOI, it provides a promising alternative for gait monitoring in frailty diagnosis. However, it also has some limitations (such as floor composition, sensors placement, gait speed, among others) that need to be addressed in order to obtain a full picture of how VBOI can be applied in frailty diagnosis.

1.2 Thesis Contribution

As mentioned previously, one of the proposed applications of VBOI is in healthcare [9, 38]. Room occupant localization techniques are one of the most researched areas in VBOI, but such methods have some limitations when running outside controlled settings. For example, most of the gait analysis studies in VBOI have been conducted with healthy gait alone, which indicates a need to investigate the performance and applicability of VBOI in frail gait [39]. Therefore, the main contribution of this thesis is an analysis of the applicability of current

VBOI techniques in a healthcare setting, particularly in human frailty diagnosis which is highly dependent on gait analysis.

1.3 Thesis Outline

In Chapter 2 a detailed review of current frailty definition and diagnosis methods is presented along with a review of VBOI algorithms for gait parameter extraction.

Chapter 3 demonstrates an application of VBOI in extracting gait features for frailty analysis and a discussion on their performance and limitations.

Chapter 4 presents the results from frailty gait analysis via VBOI.

Finally, Chapter 5 summarizes all contributions and discusses the future of VBOI algorithms in assisting frailty diagnosis.

1.4 Goodwin Hall and VBOI

One of the research fields in IoT is the study of smart buildings [46]. Such buildings contain various sensors mounted to their structure, thus creating the possibility to investigate how they respond to changes in their environment. Virginia Tech's campus is home to Goodwin Hall (GH), a 160,000 ft^2 five-story classroom structure that is equipped with 225 high sensitivity accelerometers permanently installed to its structure. GH's vibration sensors can measure vibration signals with frequencies ranging from 0.06 Hz to 10 kHz and allow for real-time measurement of the building's response. GH has been used in the development of multiple VBOI algorithms [9, 10, 11, 38, 50, 51] and structural health monitoring applications [63]. Experiments performed in Chapter 3 were conducted at GH, however, GH's underfloor

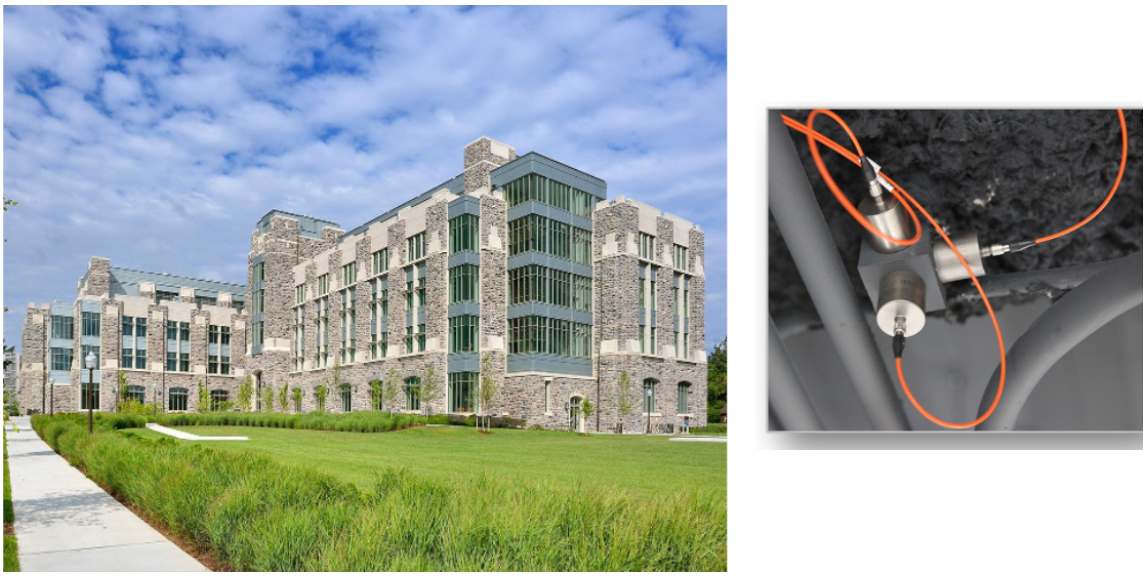

Figure 1.1: Picture of Goodwin Hall (left) with a picture of sensors used to measure vibration in three dimensions (right).

sensors were not used as this study was meant to simulate a trial at a real healthcare facility (which most likely would not have underfloor accelerometers).

Chapter 2

Literature Review

In addition to the introduction in Section 1.1, more details about the frailty criteria and gait analysis are described here. Section 2.1 describes the relationship between gait and frailty as well as the importance of gait parameters in frailty diagnosis. Section 2.2 deals with the current technologies used in the literature for measuring these gait features. Lastly, Section 2.3 describes some of the most common localization algorithms in VBOI.

2.1 Frailty and Gait

Currently, there is not a unifying definition or means of measuring frailty, in spite of its clinical significance in the healthcare sector. Defining frailty is a hard problem in the medical community because of the variety of causes and symptoms it can inflict on a patient. Some definitions propose that a recent decline in the cognitive functions combined with body and behavior changes are important elements of diagnosing frailty [32], while others prefer to take into account early- and mid-life weights on a frailty status later in life [69]. However, many of the frailty criteria in the literature focus on 6 main domains: physical conditioning, gait speed, mobility, nutrition, mental health, and cognitive abilities [60, 69]. This section provides a literature review of frailty and how gait is related to it.

2.1.1 Defining and Measuring Frailty

The consequences of frailty are well known in the literature. Patients who suffer from it have a higher chance of death in five years following the diagnosis, regardless of age [68]. Also, when compared to healthy patients, frail ones who had surgery are less likely to be discharged [55] and have a higher chance of being readmitted in the following 30 days from hospital release [56], both of which increase healthcare costs. In fact, frail elders account for the highest healthcare costs in developed countries [29].

One of the most used frailty definition is given by Fried et al. [32], which was based on a study with a sample size of over 10,000 people from the Cardiovascular Health Study (CHS). The defining frailty factors assessed by the CHS are weight loss, weak grip strength, exhaustion, slow walking speed, and low physical activity. The authors defined as "frail" anyone who exhibits 3 or more factors and as "pre-frail" those who exhibit 1 or 2 factors. Frail individuals had a rise in negative outcomes such as an increase in falls, hospitalizations, and death. Although Fried's frailty index is widely used in research, some argue that this frailty criteria has not been proved effective in the clinical setting because it fails to take into consideration the patient's cognitive functions [58]. Ávila Funes et al. [81] accounted for this by adding a cognitive impairment assessment to Fried's criteria. Their 4-year-study with over 6,000 elderly community-dwelling participants improved the frailty classification by 22% by performing the cognitive test. Rothman et al. [62] added to both studies by also considering depression symptoms and concluded that cognitive impairment, slow gait speed, and low physical activity as the key indicators of frailty. Similar criteria can be found in [27, 54, 59, 71].

A deeper definition of frailty can be found in Rockwood et al. [57] where the authors developed a frailty classification index during the Canadian Study of Health and Aging (CSHA).

Their approach relied both on a rule-based classification (just as Fried's index does) and on a clinical evaluation by healthcare professionals. Those participating in this study had to perform different clinical evaluations to get their frailty scores, which include a Modified Mini-Mental State Examination [7], indicating cognitive impairment, a Cumulative Illness Rating Scale [23], to detect comorbidities, and a CSHA-developed test to measure the patient's level of independence to perform daily living activities. Researchers also checked the participants' history of falls, delirium, or dementia. The result of this 5-year study with over 2300 people resulted in the CSHA Clinical Frailty Scale, a list of 70 disorders to be evaluated by a healthcare professional in order to detect a patient's frailty score from 1 (very frail) to 7 (very fit). Other more in-depth clinical frailty assessment criteria can be found in [36, 52, 61].

More recently researchers have proposed classifying frailty via machine learning as it has the potential of accelerating frailty detection [72]. A comprehensive paper is given by Tarekegn et al. [73] in which the authors used a health database with over 1 million entries for elderly people to run different machine learning models for frailty prediction, of which the artificial neural network and support vector machine ones performed the best. Similar results were obtained by Bertini et al. [16] using a regression model with socioclinical databases with over 95,000 entries representing the entire elderly population of Bologna, Italy. In Williamson et al. [77] a frailty validation method using machine learning was created but performed poorly, having both low sensitivity and specificity. In spite of the potential benefits of machine learning in frailty detection, this has proven to be a hard problem to solve primarily because of the complexities involved in frailty detection [16]. Other reasons for the low performance of machine learning models can be attributed to the loose definition of frailty itself [77].

However complicated defining frailty is, one thing is common in the literature: gait metrics

are powerful predictors of negative outcomes in health [65]. This is the reason why most of the research papers in this field include some gait-related criteria when deciding the best way to detect and measure a frailty status [30]. The reasons why gait analysis is important and which parameters are effective in frailty research are explored next.

2.1.2 Gait Analysis in Frailty Detection

Gait is a complex process in which different areas of the body must work continuously and synchronously in order to be performed properly [53]. This complexity in turn can be used as a way of representing people since no two human beings walk exactly the same way [35]. In fact, every time someone takes a step, a vast amount of personal information is transmitted to the environment in the form of footstep-generated vibration waves. If this person happens to be walking in a smart building, VBOI techniques could be used to extract the information contained in the footsteps. For example, Bales et al. [15] were able to detect an occupant's biological gender using underfloor accelerometer measurements, while Alajlouni and Tarazaga [10] were able to localize and track room occupants by their footstep-induced vibration waves. Unsurprisingly, fields such as biomechanics and kinesiology looked at links between gait variations and health status. These studies found that the way a person's gait changes over time can be an indication that an underlying health condition is present [35], making gait analysis an excellent tool for the early detection of health problems. To facilitate the discussion of how frailty and gait are linked to each other, Table 2.1 has the definitions of some gait parameters mentioned in the literature, and Figure 2.1 describes the human gait cycle.

Table 2.1: Definition of gait parameters.

Parameter	Definition	Reference
Gait cycle (GS)	Period between two identical events during normal walking	[53]
Single limb support	Period in which only one foot is in contact with the floor during walking. Measured as a percentage of the gait cycle	[53]
Double limb support	Period in which both feet are in contact with the floor. Measured as a percentage of the gait cycle	[53]
Gait speed	Distance traveled divided by the walking time	[13, 35]
Cadence	Number of steps per minute	[35, 44]
Step length	Distance between consecutive toe offs and heel strikes of opposite legs	[35]
Step width	Mediolateral distance between the feet during double support	[35]
Stride length	Distance between two consecutive heel strikes of the same foot	[35]
Stride time	Time between two consecutive heel strikes of the same foot	[27]

Gait speed has been the most tracked gait parameter for frailty detection [65]. Because gait speed is a quick, inexpensive, and robust measure of a patient's health, it is widely recorded by healthcare workers to determine the health status of individuals [75]. There is a particular interest in the connection between slow gait speed and frailty. Pamoukdjian et al. [47] found in their literature review that slow walking speed alone over a short distance (about 4 meters) is better at identifying medical complications related to frailty than more advanced walking and cognitive tests for those over 65 years old. Similarly, in their review paper, Liu et al. [42] reported that slow gait speed was associated with a higher risk of death

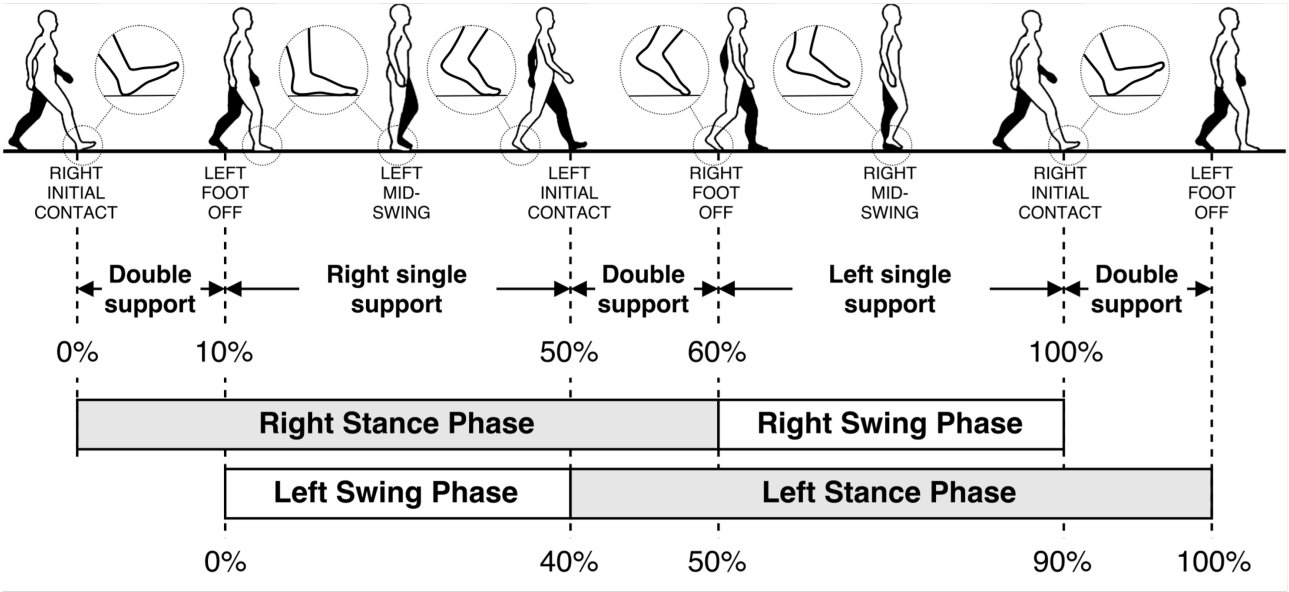

Figure 2.1: Human gait cycle [74]

for the elderly. Slow gait speed can also tell the presence of certain types of cancer [18], cardiovascular disease [8], and chronic kidney disease [79].

However, some authors argue that gait speed should not be used as the only discriminating gait parameter between frailty levels because it is also linked to other aging-related health problems and does not provide, by itself, a deep insight into gait patterns [65]. Therefore, combining gait speed with other gait parameters can increase the performance to identify frailty. For example, Schwenk et al. [65] reported in their extensive review paper that slow cadence was a factor to distinguish between non-frail and pre-frail individuals in many studies. da Silva et al. [24] conducted a study with 125 community-dwelling elderly participants in Brazil and found that cadence discriminated between pre-frail to frail and between non-frail to frail. However, when analyzing gait differences between pre-frail and frail individuals, Freire Junior et al. [31] did not find evidence that cadence is a strong discriminating factor but variations in gait were.

Stride-to-stride variability, measured by the Coefficient of Variation (CV) (Equation 2.1),

measures the repeatability of coordinated steps during steady-state walking [45]. Low variability means that steps are automatic and do not require extra effort and it has been linked to adequate gait control [34]. On the other hand, high gait variability can be a predictor of health problems (e.g., falls) even better than gait speed in some cases [17, 45]. An excellent study of stride variability and its association with frailty is given by Montero-Odasso et al. [45]. In this paper, the authors measured the frailty status of 100 community-dwelling participants using Fried's criteria and used a multivariate linear regression model to find the associations between frailty and gait variability. Their results show that variability in stride time, stride width, and stride length are associated with frailty but not double support time [45]. Interestingly, their paper also claims that variability in some gait parameters has an association with frailty regardless of gait speed as long as patients walked as fast as they safely could. They argue that this happens because walking at a fast pace induces a higher degree of effort, which facilitates the measuring of gait variability due to frailty [45].

$$\text{CV} = \frac{\text{Standard Deviation}}{\text{Mean}} * 100\% \tag{2.1}$$

2.2 Gait Data Acquisition in Frailty Research

There are multiple ways to obtain gait data needed for frailty analysis in the literature. Those range from simple and affordable methods (e.g., stopwatches) to more advanced and expensive ones (e.g., force plates). This section will review some of the most commonly used ones in both the literature and the medical community to analyze their performance based on ease-of-use, cost, and the capability to measure different gait features.

2.2.1 Stopwatch Measurements

Section 2.1.2 detailed the importance of measuring gait speed in frailty detection. However, it is common practice to measure gait speed with a stopwatch over a predefined distance during clinical evaluations in healthcare [30]. Although stopwatches are highly affordable and easy to use, the main disadvantage over this procedure is that their time measurements are subject to both intra- and inter-observer variability, as different health professionals will most likely disagree on the exact moment that patients finished their walking trial [30, 66]. Additionally, stopwatch measurements are usually limited to only obtaining gait speed even though it would be beneficial to track other gait parameters as well to aid the frailty diagnosis. Furthermore, many attempts have been made in the literature to develop more robust systems to replace stopwatches during frailty evaluations.

2.2.2 Force Plates and Mats

Different studies found in [24, 31, 41, 45] used sensorized mats or plates during walking trials. Such devices are known for their reliability and validity as mentioned by McDonough et al. [43], where they found the commercially available pressure mat GAITRite [2] to be 99% as accurate as motion capture devices. However, pressure mats are costly and not easy to calibrate and use, which hinders the accessibility of such technology [30]. Another issue with pressure sensing mats/plates is that they need to occupy a large area (Fried recommends a walking trial of at least 4 meters in length [32]) to be effective for gait analysis in frailty, making them nonviable in many settings [33], especially in smaller healthcare facilities or at patients' homes.

2.2.3 Motion Capturing Systems

Motion capture devices provide an alternative to pressure mats while still producing highly accurate tracking results without the need to occupy a large area. These setups are considered the gold standard for gait analysis and have even been used in the video-game industry for capturing more natural body movements [12, 41]. However, systems like the Vicon [5] are expensive and require a specialized setup in a gait analysis laboratory as well as a time-consuming marker placement on the participants [12]. More affordable options include the Microsoft Azure Kinect [4] which can automatically detect and track up to 32 different body parts and does not require the use of reflective markers. For this reason, the Azure Kinect has been used in several studies for in-home gait monitoring to assess fall risks [70]. The main disadvantage with camera-based gait analysis has to do with privacy concerns as cameras are able to record both video and sounds from patients and those around them.

2.2.4 Wearables Systems

Wearable technologies provide benefits to many areas of healthcare monitoring since these devices are usually easy to operate and highly affordable. They can also be used to track patients outside healthcare facilities and share real-time health information with healthcare providers, thus enabling continuous patient care [28]. Such devices include smartwatches, IMU sensors, shoe pressure switches, among others. The review paper in [40] shows that in spite of the recent growth in popularity, smartwatches have only been used a few applications in healthcare research, most of which focused only on the feasibility of these devices in healthcare research. Therefore, this field of study still needs to be better explored. Wearables face a major drawback when it comes to personal privacy because they can be used to track features unrelated to health. For example, most of the devices that communicate over the

internet can secretly share users' location via GPS to the internet provider or consumer marketing agencies. Wearable technologies also rely on the patient to attach them, which can be uncomfortable and inconvenient, assuming the user remembers to use them in the first place.

2.2.5 VBOI in Gait Analysis

A network of floor-mounted accelerometers has been proposed as an alternative to extracting gait features without having to access any other patient data. These devices do not need an extensive setup process and can also be used for other applications, such as structural health monitoring [38]. The usability of accelerometers in gait monitoring rests on their performance to determine not only *when* an event happened (which is relatively easy to do), but also *where* it happened (a more complicated problem). Thus an overview of common footstep detection and localization algorithms in VBOI is presented in the following sections.

2.3 Localization Algorithms in VBOI

Localization of room occupants based on footstep-induced waves is one of the most explored topics in VBOI. These techniques use a network of sensors to measure the vibration generated by footsteps and use that information to estimate the footstep location. Two of the most common types of localization algorithms include time-of-arrival and energy-based ones.

2.3.1 Time-of-Arrival Methods

Time-of-Arrival (TOA) relies on accurately measuring when a wave arrives at a sensor. If more than one sensor is used, it is possible to calculate the time difference of arrival (TDOA)

and thus obtain an estimate of the source location [14]. For example, assuming some footsteps happen near an array of N sensors where the N^{th} sensor is considered the reference one, then the traditional TDOA algorithms work by simultaneously solving a system of $N-1$ hyperbolic equations described by:

$$d_i - d_N = v \times (TDOA)\,, \tag{2.2}$$

where $d_i = ||\mathbf{r}_i - \mathbf{r}_s||$ is the distance between the footstep location ($\mathbf{r}_s$) and the sensor ($\mathbf{r}_i, i = 1, 2, ..., N-1$), d_N is the distance between the footstep and the reference sensor, and v is the estimated wave speed. Then Equation 2.2 can be solved for the source location $\mathbf{r_s}$.

An efficient localization algorithm assuming constant wave speed was developed by Chan and Ho [19]. In their study, they linearize the TDOA nonlinear system of equations by adding an intermediate variable. The source location was then determined using a least-squares algorithm. Results from [50, 64] show that the algorithm developed in [19] had a range of accuracy between 2 to 10 feet in tests performed in Goodwin Hall using an impact hammer. Chen et al. [21] proposed linearizing the localization problem by adding two extra variables to the nonlinear problem. Localization estimates could then be obtained by an alternative least-squares approached named *constrained least-squares* that required only 3 sensors for the 2-dimensional localization problem. The reduction of the number of sensors is significant because the accuracy of the least-squares methods increases as the number of sensors increase.

A major assumption in TDOA algorithms is that the wave speed is constant, which means that the wave travels through non-dispersive media. However, Chen et al. [20] indicate that seismic waves decay rapidly, and [14] reports that the floor's dominant flexural mode is distorted as the wave travels the floor. This means that the footstep wave components with

higher frequency will travel at nonlinear speeds, thus distorting the wave [11]. The result is a loss of accuracy when detecting footsteps with traditional TDOA algorithms as different frequency components arrive at the sensors at different times [14, 51, 64].

Algorithms addressing wave dispersion and distortion have been proposed. Ciampa and Meo [22] utilize the continuous wavelet transform to increase the TDOA localization accuracy in dispersive media. This analysis looks at the TOA of the dominant frequency component of the seismic wave, rather than considering its entire spectrum. This method was reported to give location estimates within 5 millimeters of the true source location, but it is computationally expensive and the authors only tested it in controlled environments. In [14] a perceived wave propagation velocity variable is introduced and an algorithm was created based on the sign of the time difference of arrival (which splits the floor into different searching regions) to obtain better TDOA estimates. The proposed algorithm assumes that the order of wave arrival between sensors is the same independently of the dispersion to choose a region that is more likely to be the event origin.

2.3.2 Energy-Based Methods

Energy-based methods assume that the wave energy decays with distance, thus a sensor network could be used to estimate the event source location [10]. Advances in energy-based algorithms were first developed in acoustics as researchers proposed that the energy of acoustic waves advancing in free space decays proportionally to the inverse of the squared distance [49]. Other authors developed models in wireless communication based on the received signal strength (RSS), which is comparable to the amplitude of an accelerometer measurement. RSS-based localization algorithms have been well-studied in the literature, particularly in indoor localization using the Wi-Fi network [76]. RSS methods assume an

exponential energy decay, which means that the energy would be infinite if the source's location is the same as the sensor's. For example, in [49] an RSS model was created according to:

$$E(d) = E(d_0)\left(\frac{d}{d_0}\right)^{\beta}, \tag{2.3}$$

where $E(d)$ is the average RSS power, measured over a time interval, d is the distance to the source, the unknown RSS value at a distance d_0 from the source is represented by $E(d_0)$, and $\beta < 0$ is the power attenuation parameter. It can be seen from Equation 2.3 that if the source shares the exact location with the sensor, then $E(d = 0) = \infty$, which is undefined. Alajlouni et al. [11] proposed an alternative decay model to overcome this limitation presented as $E(d) = E_0 e^{\beta d}$ where $E_0 > 0$ is a scalar parameter.

Furthermore, in [10] a new algorithm for indoor footstep localization was proposed based on the decay model in Equation 2.3 as follows:

$$Q_i = Q_s e^{\beta(||\Delta \mathbf{r}_i||)}, \tag{2.4}$$

where Q_i is the measured wave power at sensor $i = 1, 2, ..., N$, Q_s represents the average power produced by the source, which is unknown, $||\Delta \mathbf{r}_i||$ is the Euclidean distance between the i^{th} sensor and the source, that is, $||\Delta \mathbf{r}_i|| = ||\mathbf{r}_i - \mathbf{r}_s||$, where $\mathbf{r}_i$ is the known location of for the i^{th} sensor and $\mathbf{r}_s = [x_s \quad y_s]^T$ is the unknown source location. Lastly, β is the wave's attenuation rate which has to be estimated during the calibration phase. Since it is hard to estimate Q_s in practice, the authors introduce a reference sensor quantity to replace it as shown in Equation 2.5:

$$Q_{iR} \equiv \frac{Q_i}{Q_R} = e^{\beta(||\Delta \mathbf{r}_i|| - ||\Delta \mathbf{r}_R||)}, \tag{2.5}$$

where Q_R is the average power measured by a reference sensor, chosen to be the sensor with the largest calculated power for each footstep, and the Euclidean distance be-

tween the reference sensor and the source is given by $\Delta\mathbf{r}_R$. Then, a system of $N-1$ nonlinear equations is generated from Equation 2.5 of the form $\mathbf{f}(\mathbf{r}_s) = 0$, where $\mathbf{f}(\mathbf{r}_s) = [f_1(\mathbf{r}_s), f_2(\mathbf{r}_s), ..., f_{N-1}(\mathbf{r}_s)]^T$, and an estimate of $\mathbf{r}_s$ (represented as $\hat{\mathbf{r}}_s$) can be obtained by solving the following optimization problem:

$$\hat{\mathbf{r}}_s = \underset{\mathbf{r}_s \in \mathbb{R}^2}{\arg\min} \, ||\mathbf{f}(\mathbf{r}_s)| \, |_2^2. \tag{2.6}$$

This work uses this algorithm in frailty gait analysis because of its proposed performance and simplicity. A more detailed study of its methods is provided in the following chapter.

2.3.3 Model-Based and Data-Driven Methods

Model-based and data-driven approaches are among the most recently developed techniques to detect and localize vibration events in a structure. One of the advantages of a model-based approach is the possibility to include the dynamics of the structure into the model, thus improving the robustness of the localization algorithms. However, model-based approaches increase computational power as models become larger and more complex. They can also introduce sources of uncertainties when combined with data from vibration sensors due to sensor resolution and precision, and model imperfections. In Drira et al. [26] a vibration-based model is used to localize and track room occupants. Their approach consists of a finite element floor model in which all possible walking trajectories are simulated. Real measurements are also taken by using vibration sensors. Both real and simulated footsteps go through a wavelet decomposition so that their low-and-high frequency components are extracted. Footsteps can then be localized by comparing the similarities between the frequency components of both the real and simulated footsteps. However, this algorithm is more focused on accurately tracking the walking direction than localizing individual footsteps.

Data-driven approaches usually rely on a previously acquired database of vibration events at different locations on the floor. An interesting localization algorithm is the Force Estimation and Event Localization (FEEL) algorithm developed by Davis et al. [25]. This algorithm utilizes the floor vibration due to an impact and a transfer function to estimate the force released by the vibration source at the impact location. The force estimate is given by:

$$\hat{f}_{ij} = \text{IFFT}\left(\frac{S_j(f)}{\hat{T}_{ij}}\right), \tag{2.7}$$

where $\hat{f}_{ij}$ is the force estimate at impact location i, IFFT() is the inverse Furrier transform, $S_j(f)$ is the floor vibration measured at position j, and $\hat{T}_{ij}$ is the transfer function.

Therefore, it is possible to localize a vibration source by comparing its force estimate $\hat{f}_{ij}$ to the ones obtained during the calibration phase at different points on the floor. The advantage of the FEEL algorithm is that it does not depend on the distance between the impact point and the sensor location, thus eliminating the need to synchronize the sensors. However, this algorithm relies on a database of force estimates obtained during the calibration phase. Thus, it will give unreliable estimates for events that occur in locations not tested during calibration.

Chapter 3

VBOI-Based Footstep Localization

This chapter provides an experimental application of the energy-based footstep localization algorithm described in Section 2.3 in gait analysis for frailty diagnosis.

3.1 Methodology

The experiment described in this chapter took place in Goodwin Hall (GH) at Virginia Tech's campus. There are 225 high sensitivity accelerometers permanently mounted to the structure of GH which continuously monitor the building vibrations due to its occupants and the environment. Many of the previous VBOI algorithms mentioned in this study have been tested at GH [11, 50, 51, 78]. However, since this study was supposed to simulate a real hospital setting, it was decided to manually mount 6 PcB Piezotronics model 393B04 accelerometers on a hallway on the 4^{th} floor of GH. These accelerometers can measure accelerations within the bandwidth of 0.06-450 Hz, and have a sensitivity of 1,000 mV/g (g = $9.81 m/s^2$) [6]. A schematic of the sensors' layout is shown in Figure 3.1.

A Microsoft Azure Kinect, capable of performing body tracking as mentioned in Section 2.2, was used for reference. The camera was mounted approximately 1 meter above Sensor 1, facing the remaining accelerometers as shown in Figure 3.2. The Azure Kinect contains a 1 MP infrared depth camera based on the time-of-flight principle and is capable of taking depth measurements accurately up to 5.46 meters away [4]. It also contains a 12 MP RGB

camera, a 7-microphone array, and an integrated IMU. An app was created using the Body Track SDK version 1.0.1 developed by Microsoft [4] to track test participants at 30 frames-per-second using only the depth camera in the narrow field-of-view settings, which allows for the greatest tracking distance from the camera.

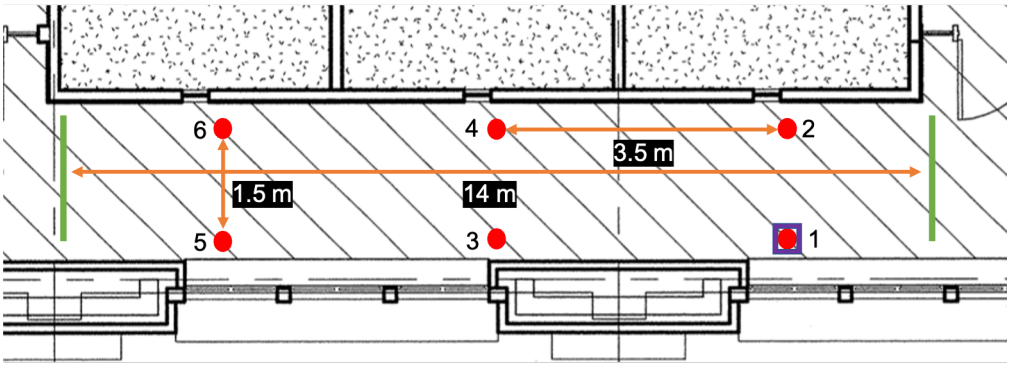

Figure 3.1: Floor section in Goodwin Hall where the experiment took place. Dots represent accelerometers mounted on top of the floor, the Azure Kinect is represented by a square, the starting/ending walking points are shown by green lines. Note: image not to scale.

Figure 3.2: Photo of the sensors' layout during the experiment.

A total of 2 healthy male individuals wearing regular shoes, and 1 healthy male individual wearing soft-sole shoes participated in this experiment. Before each trial, participants were

briefed to start walking down the hallway only after receiving a vocal command and to start with the left leg first. They were also told to stop walking as soon as they reached the finishing line to not inadvertently excite the accelerometers with extra steps. Two walking scenarios were tested at both usual and fast gait speeds: one at body weight and another with a 5 pound (2.268 kg) weight added to one of the participants' ankles. Adding the extra weight only to one leg made it harder to walk along the hallway, thus it was found to be an adequate method of simulating frailty. "Fast gait" was defined as a brisk walk but without running, while "usual gait" or "regular gait" was the normal walking speed for each participant. Once completing the walk in one direction, participants lined up again at the finish line and the process was repeated. A total of 4 walking trials for each walking scenario (regular and fast gait at body weight, and regular and fast gait with added weight) were completed, totaling 12 walking trials for each scenario.

Participants were also asked to perform walking trials in which they had to step at specific spots down the hallway so that the accuracy of the localization algorithm could be measured. Marked footsteps had a length of approximately 0.70 meter, or 20 footsteps for the entire walk. Finally, 4 stopwatch measurements were taken for each trial (every time the participant passed by a sensor and when he reached the finish line) using a stopwatch from an iPhone XS running iOS 14 from Apple [1]. It was hypothesized that the added weight would produce a significant difference in the tracked gait parameters when compared to walking at body weight.

It is worth mentioning that this experiment was conducted later in the day to prevent sources of noise and uncertainty during the trials. These include other people walking near the hallway, doors opening/closing, printers working, and even heavy traffic in the road next to GH.

3.2 Footstep Localization

This section describes the techniques used for localizing footsteps using an energy-based algorithm. First, the time-varying power of the vibration signal is calculated in order to detect footsteps. Once detected, footsteps are localized according to the algorithm described in Section 2.3.2. Finally, a technique for detecting and localizing footsteps from the Azure Kinect is discussed.

3.2.1 Footstep Detection Using Accelerometers

Although there are multiple methods for detecting acceleration signals that look like a heel strike, the one used in this study is similar to the one proposed in [38], which detects heel strikes as peaks in the energy of the acceleration signal. First, the acceleration signal is broken into time windows of approximately 0.02 second, then the average power of each window is computed according to:

$$Q_i(t_{0i}, t_{pi}) = \frac{1}{t_{pi} - t_{0i}} \int_{t_{0i}}^{t_{pi}} Z_i(t)^2 dt. \tag{3.1}$$

Let $\mathbf{Q}_i$ be a vector of length M containing the average power of every window, in sequence, at sensor i during a measurement period. The signal-to-noise ratio (SNR) is defined as the ratio between two consecutive elements of $\mathbf{Q}_i$ as described by Equation 3.2:

$$\mathrm{SNR}_{i(n)} = \frac{Q_{i(n+1)}}{Q_{i(n)}}, \tag{3.2}$$

where $n = 1, 2, 3, ..., M - 1$. Since the power of random noise in the measurement is close to 0, the SNR will peak when a footstep happens. Therefore, it is possible to detect a footstep

by searching for peaks in the SNR that are above a certain threshold as shown in Figure 3.3.

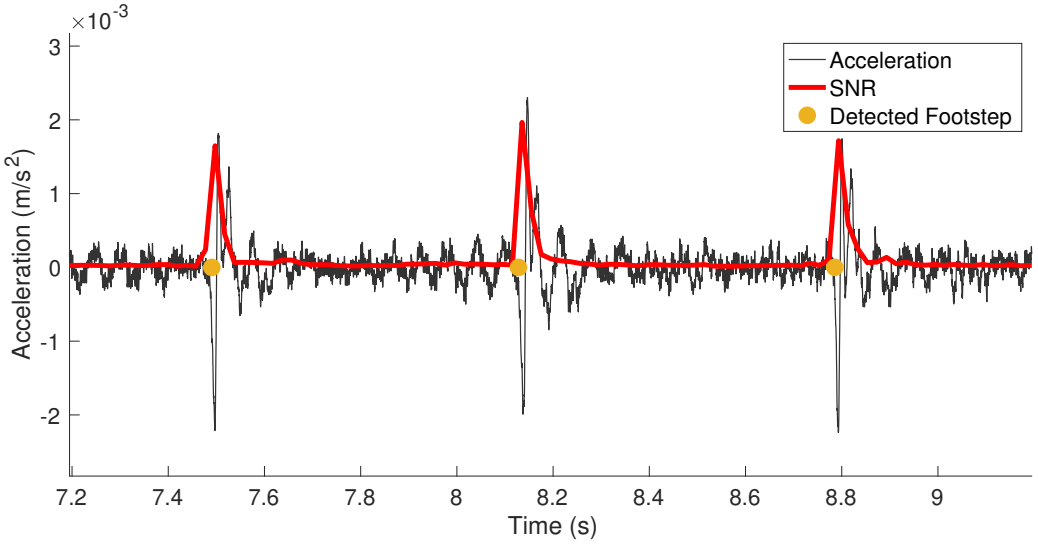

Figure 3.3: Example of three detected footsteps based on peaks in the SNR.

It is interesting to note that this algorithm is more effective when participants walked at fast gait speed. This happens because there is an increase in footstep energy when participants walk faster [38], thus making their detection easier when compared to noise in the acceleration signal as shown by Figures 3.4 and 3.5.

3.2.2 Energy-Based Footstep Localization

The amplitude of the acceleration signal increases as a participant continually moves towards a vibration sensor. In fact, the measured floor acceleration will reach its maximum when the participant is the closest to the sensor. For example, if a person walks the closest to the i^{th} sensor, then that sensor will have the highest calculated average power. Using this information, Alajlouni and Tarazaga [9] developed a fast technique to roughly locate

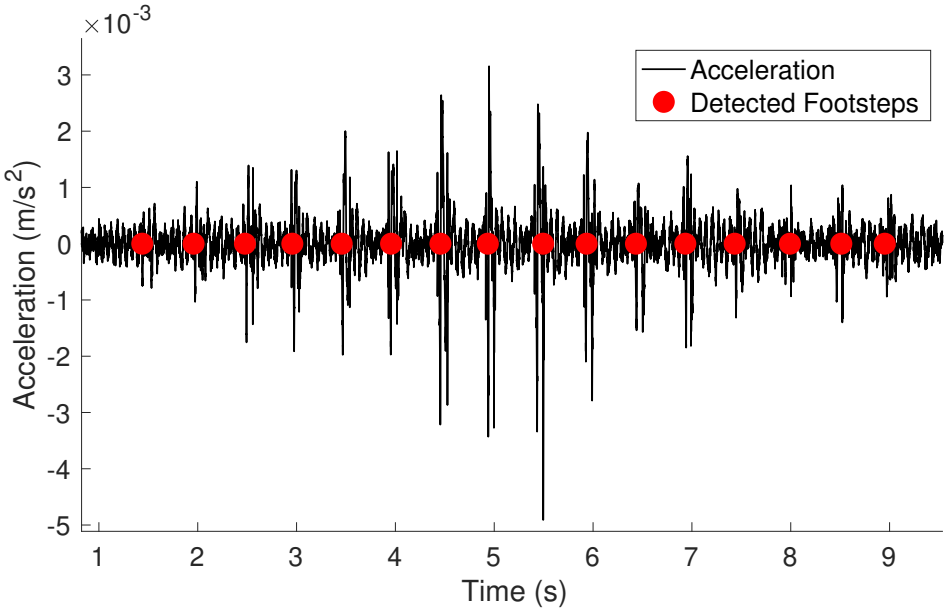

Figure 3.4: Example of acceleration signal at fast gait. It can be seen that the detected footsteps have clearer peaks above the noise level. This does not happen in Figure 3.5 where the algorithm was not able to accurately differentiate between noise and footsteps.

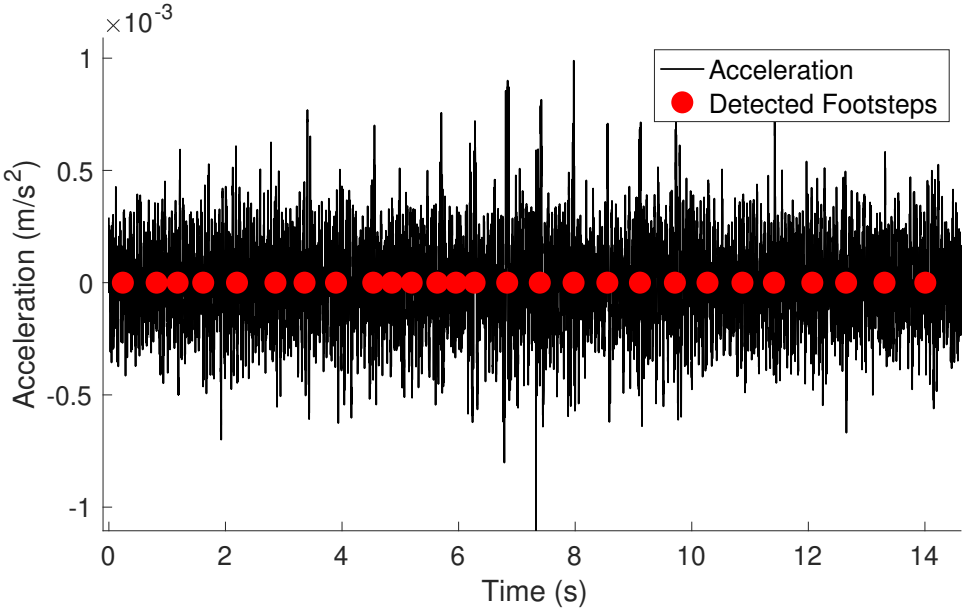

Figure 3.5: Example of acceleration signal at slow gait. This is an example of the worst-case scenario for the footstep detection algorithm, which is when the walker is wearing soft-sole shoes and walking relatively slowly.

footsteps by weighing each sensor location to the corresponding footstep average power Q_i and then summing the sensor-weighted locations as shown in Equation 3.3:

$$\hat{\mathbf{r}}_s = \frac{\sum_{i=1}^{N} Q_i \mathbf{r}_i}{\sum_{i=1}^{N} Q_i}, \tag{3.3}$$

where $\hat{\mathbf{r}}_s = [\hat{x}_s \quad \hat{y}_s]$ is the estimated 2-dimensional footstep location, r_i is the sensor location, and Q_i $(i = 1, 2, ..., N)$ is the calculated footstep average power. Figure 3.6 shows an example of the rough localization results.

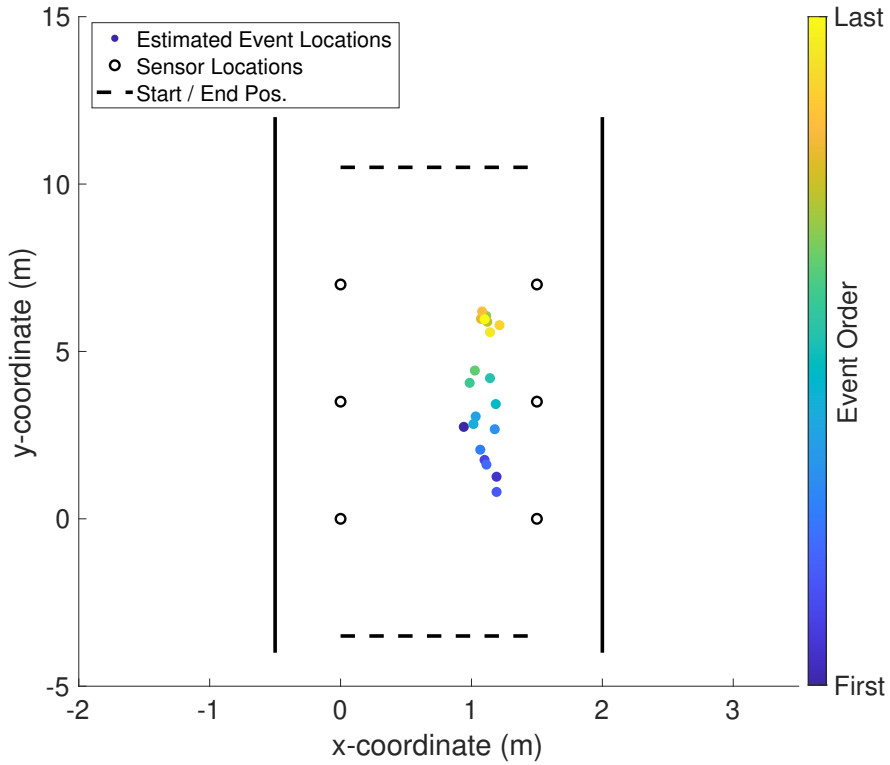

Figure 3.6: Example of a footstep localization trial using the heuristic sensor-weighted approach.

An important limitation of the heuristic algorithm can also be seen in Figure 3.6: the estimated position footsteps are more accurate for the ones that happened inside the convex-

hull of the sensor location points. The convex-hull is the smallest convex geometry that contains all sensors as seen in Figure 3.7.

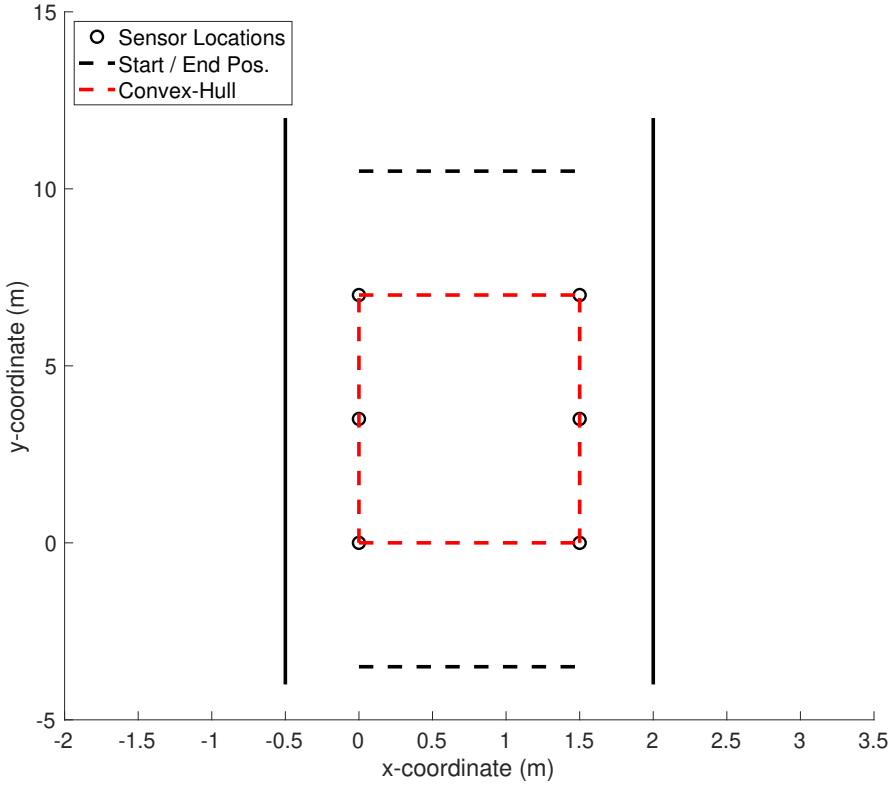

Figure 3.7: Convex-hull of sensors.

The results from the heuristic localization algorithm can be used as starting points for the nonlinear optimization problem from Equation 2.5. The algorithm chosen to optimize the $N-1$ nonlinear system of equations described by Equation 2.6 was the *trust-region-reflective* provided by MATLAB version R2020b [3]. The boundaries given for the nonlinear solver were from 0 to 1.50 m in x and from -3.5 to 10.5 m in y (Figure 3.6). The accuracy of the localization algorithm can be measured by the mean absolute error (MAE) given by $\text{MAE} = \sqrt{\frac{\sum_{k=1}^{N} ||\epsilon_k||}{N}}$, where ϵ is the error or difference between the true and estimated footstep position and N is the total number of footsteps.

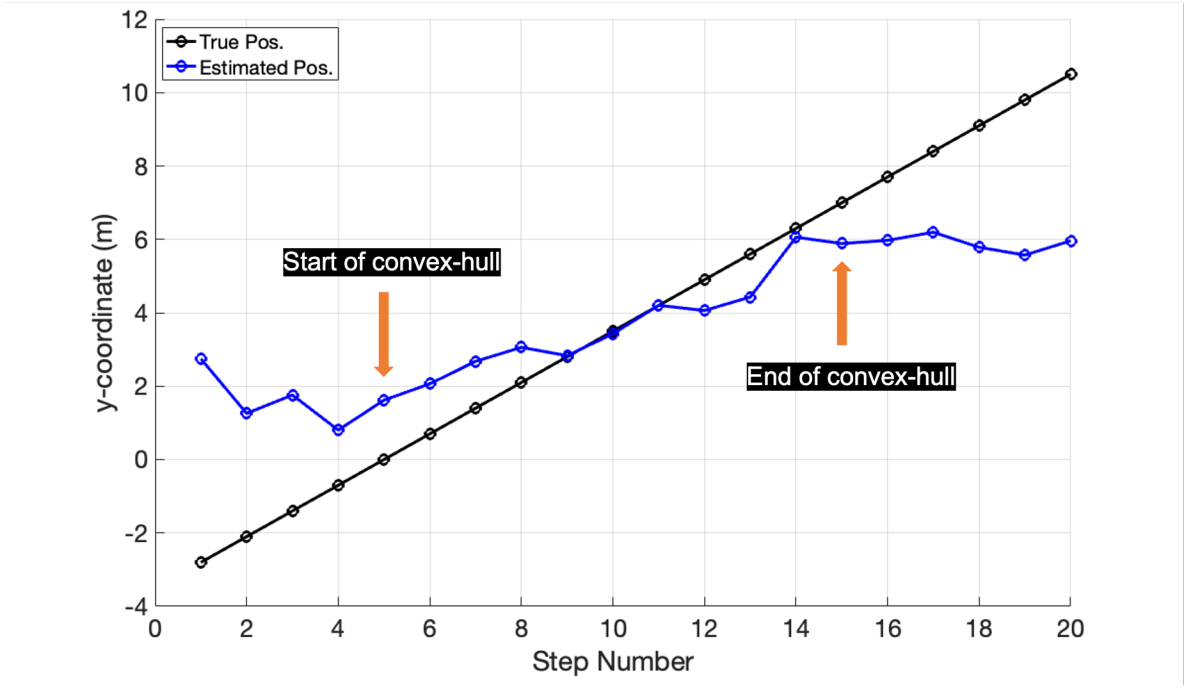

Figure 3.8: Plot of the estimated footstep localization using the heuristic sensor-weighted algorithm in the walking direction. The MAE for the entire walk is 2.20 meters while the MAE in the convex-hull is 0.98 meter.

As mentioned previously, the introduction of a reference sensor in Equation 2.5 replaced the need to estimate Q_s. However, the energy decay parameter β still needs to be calibrated on-site. The calibration process takes into consideration that higher frequency components of the footstep acceleration signal decay faster (e.i, β has a lower value) [14]. Alajlouni et al. [11] showed that hammer impacts proved to be an adequate method of obtaining a lower bound for β because such impacts contain higher frequencies components than footsteps. Their results provided an appropriate range for β on the 4^{th} floor of GH is $-0.75 < \beta < 0$. These were the values used for the decay parameter in this study. An example of an improved localization trial is shown in Figure 3.9 while Figure 3.10 plots the estimated and true footstep positions for comparison.

Given the algorithm's limitations to localize footsteps outside the convex-hull, it was decided to only use detected footsteps inside of it when calculating gait features. Doing so not only

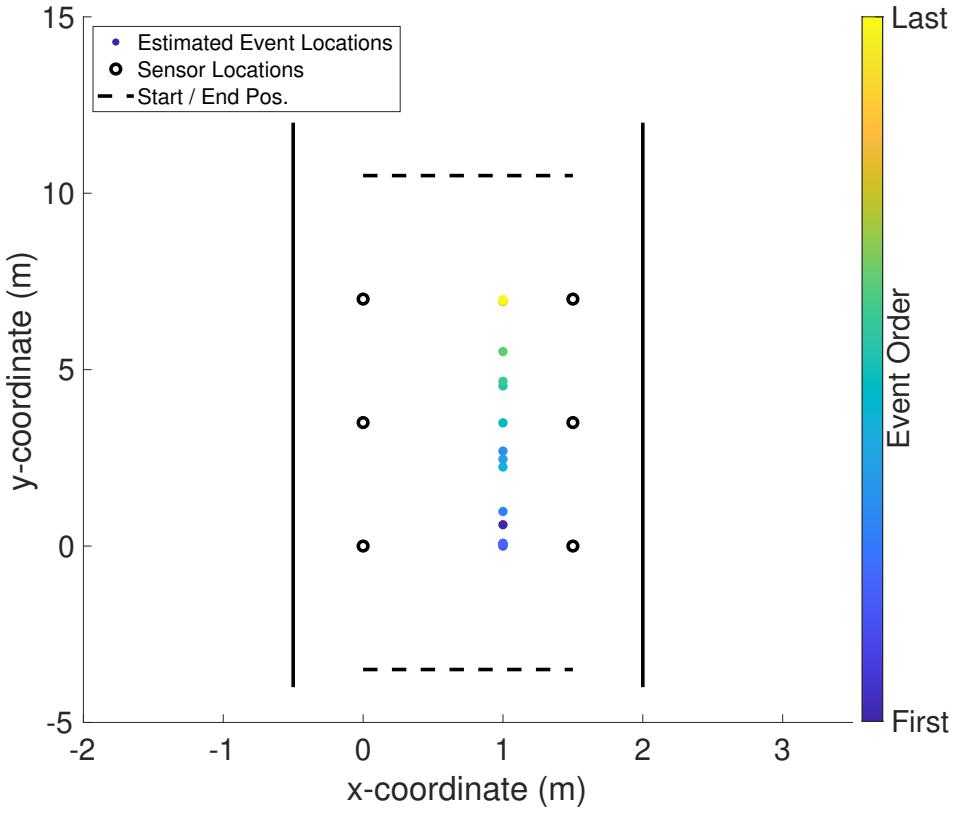

Figure 3.9: Localization results the same walking trial in Figure 3.6.

improves the spatial accuracy but also makes sure that such parameters are obtained during the steady-state walking phase as different studies proposed [32, 41, 47, 65]. Finally, a summary of the energy-based footstep localization algorithm is provided by Figure 3.11.

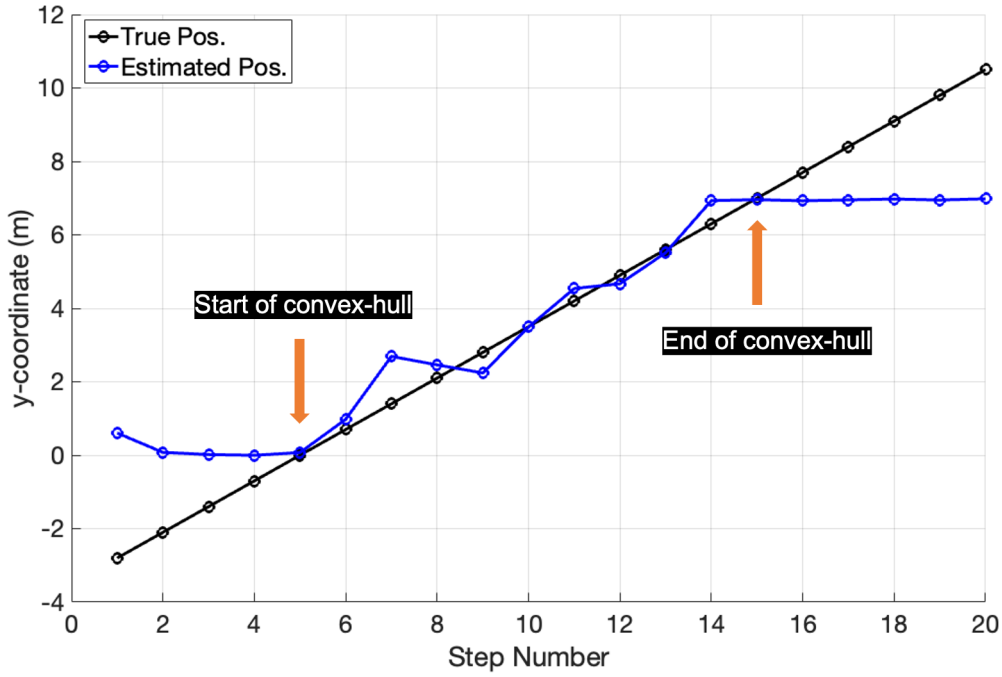

Figure 3.10: Improved footstep localization plot in the walking direction. The MAE for the entire walk and the convex-hull are 1.57 meters and 0.50 meter, respectively.

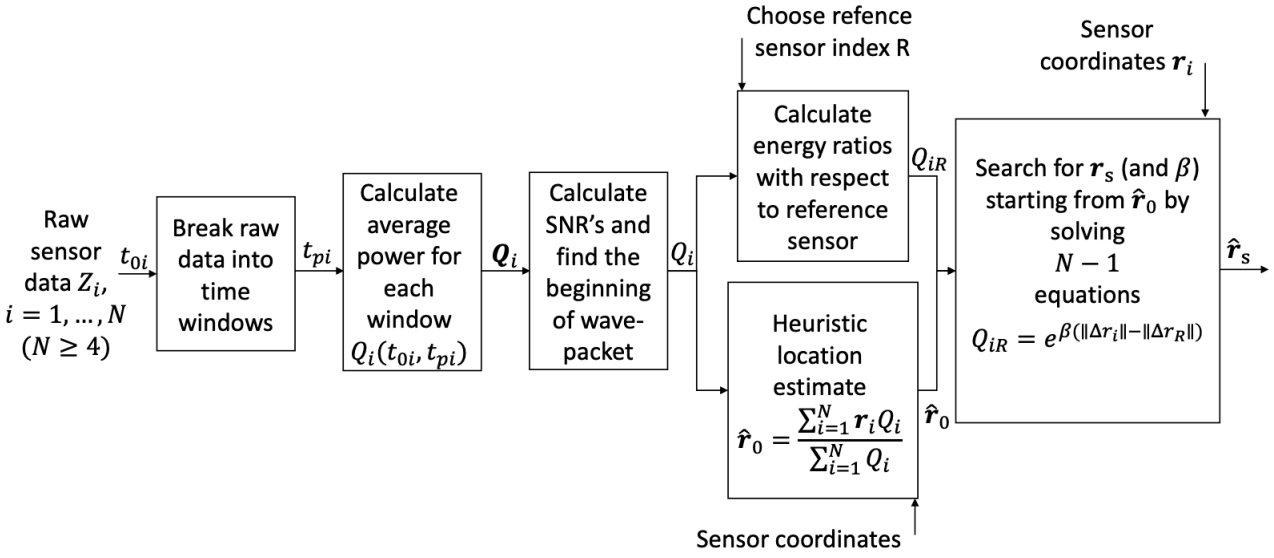

Figure 3.11: Summary of the localization algorithm used in this study [10].

3.2.3 Footstep Localization Results

As mentioned previously, a total of 20 footsteps (each with approximately 0.70 meter in length) were marked along the hallway. Participants were asked to walk at a regular speed while trying to step on each mark as accurately as possible, totaling 560 steps. The calculated MAE's for the entire walk were 0.74 m and 1.60 m in the x and y directions, respectively. Considering only footsteps in the convex-hull, the MAE becomes 0.75 m in the x-direction and 0.85 m in the y-direction. Figures 3.12 and 3.13 show the localization errors per footstep location.

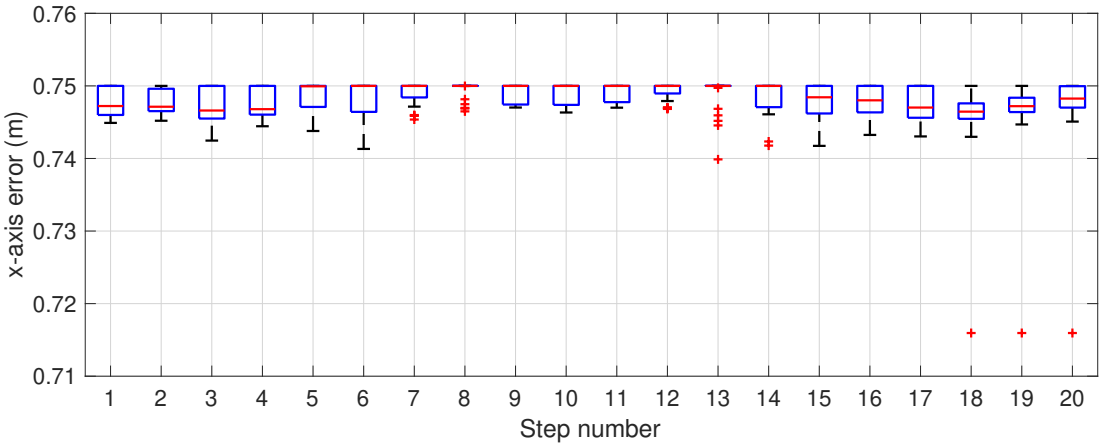

Figure 3.12: Localization errors in x at each footstep location.

It can also be seen that footsteps in the x-direction were biased towards the sensors placed further away from the structural wall of the hallway. By being closer to the structural joint between the wall and the floor, sensors 1, 3, and 5 could have been placed in a stiffer floor section than the remaining sensors. The disparity in floor stiffness could distort the seismic waves differently, causing signals arriving at sensors closest to the wall to have less energy than those arriving at sensors further away. Furthermore, the mean Euclidean norm of the error $||\epsilon|| = ||\hat{\mathbf{r}} - \mathbf{r}_{true}||$ (error distance) between the estimated footstep location and the true one is 1.23 meters.

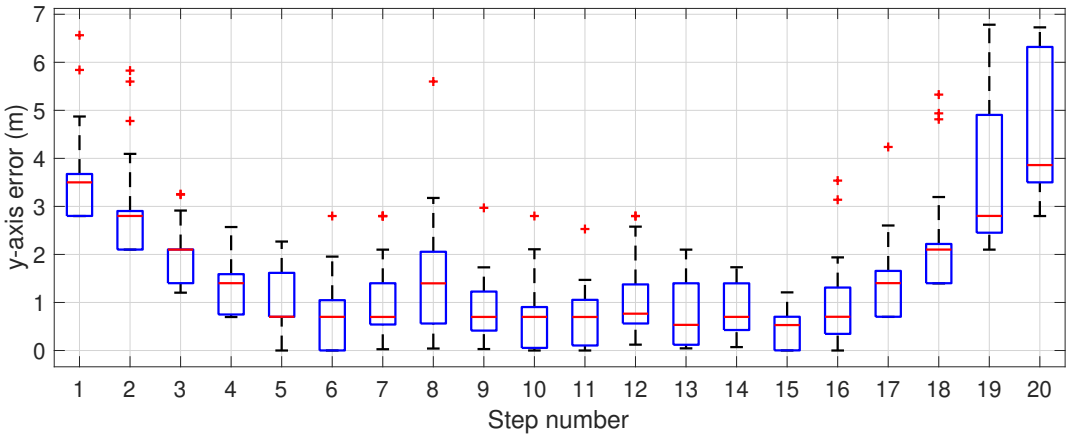

Figure 3.13: Localization errors in y at each footstep location.

3.2.4 Footstep Detection and Localization Using the Azure Kinect

The Azure Kinect camera can simultaneously track the position of up to 32 different points (named joints) in the body as shown in Figure 3.14a. The camera's coordinate system is defined in Figure 3.14b. Since the camera was positioned at an angle in relation to the walking direction, it was necessary to adjust the camera's depth measurements in the z-direction to the true walking distance vector located in the middle of the hallway. This was done by projecting the camera measurements in the z-direction according to the Pythagorean Theorem as shown in Figure 3.15.

If the participant is traveling away from the camera, the distance between the camera and the ankle joints will steadily increase during the swing phase of the gait cycle. However, once a heel strike happens and a foot is in contact with the floor, its distance to the Kinect camera will remain unchanged. Therefore, it is possible to roughly estimate when a footstep happened by plotting the position of the ankle joints in the direction of travel vs. time as shown by Figure 3.16.

Then the challenge becomes precisely knowing when heel strikes (HS) and toe-offs (TO)

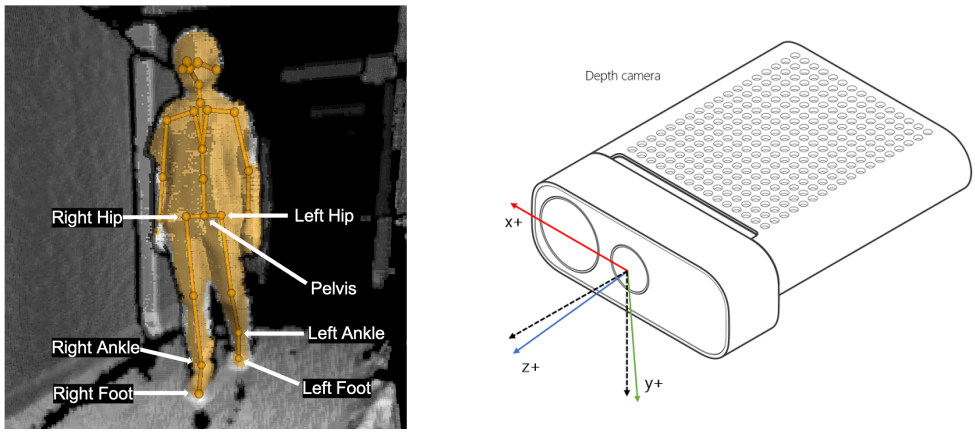

(a) Depth camera image.

(b) Azure Kinect coordinate system [4]

Figure 3.14: Example of the tracked Azure Kinect body joints (circles) and the coordinate system of the Azure Kinect. The black dotted lines in 3.14b are the coordinates of the RGB camera, which was not used in this study.

happened. In [80] a simple algorithm was created to determine gait events during treadmill and overground walking using a camera-based motion analysis system. In their experiments, participants were asked to walk at a constant speed on a treadmill, meaning that the relative distance between the participants' center of mass and the cameras was relatively constant. Thus, a plot of a foot marker in the direction of travel versus time will produce a sinusoidal curve where peaks and troughs represent HS's and TO's, respectively. In order to have the same effect during overground walking, the authors proposed subtracting the z-coordinate (direction of walk) of the sacral body marker from the z-coordinate of the heel marker at each captured frame. This process changes the coordinate system of the body markers so that they appear to be moving relative to a stationary sacral point, as if the floor was a treadmill as shown by Figure 3.17. Finally, HS's and TO's are detected according to

$$t_{HS} = (Z_{heel} - Z_{pelvis})_{max} \qquad t_{TO} = (Z_{heel} - Z_{pelvis})_{min} \tag{3.4}$$

The authors in [80] also claim that such a simple method detects gait events with a mean

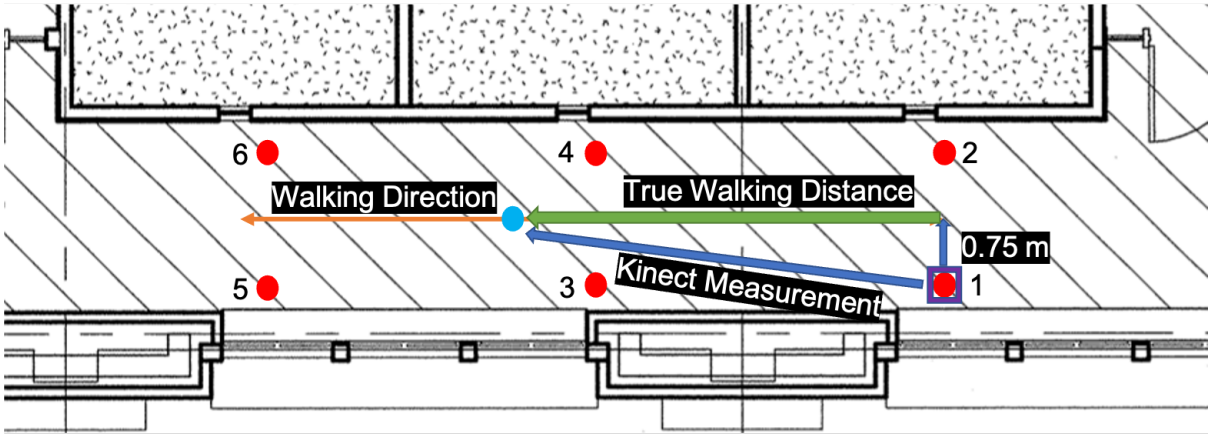

Figure 3.15: Example of adjusting the Azure Kinect's depth measurements. Accelerometers are represented by red circles while the Kinect camera and the participant are represented by a purple square on top of sensor 1 and a light blue circle, respectively.

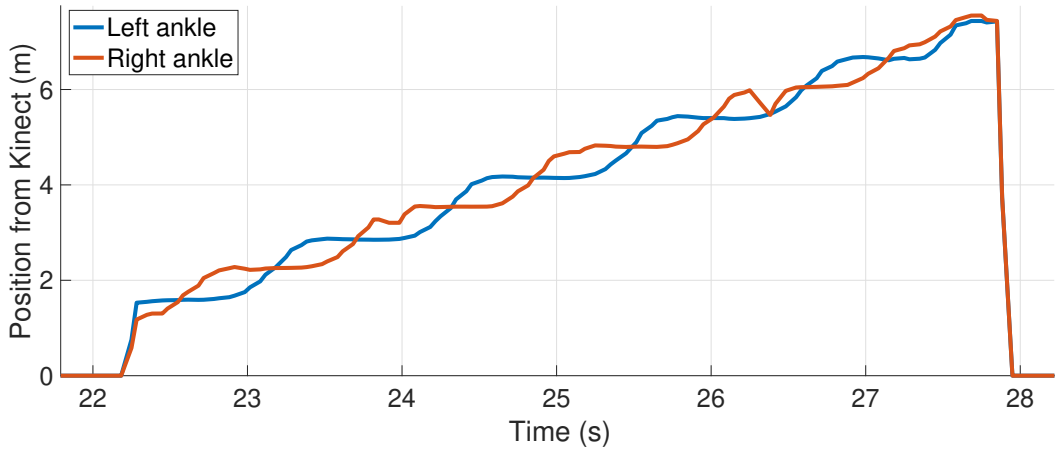

Figure 3.16: Depth camera measurements of the ankle joints. A positive slope means that the foot is in the swing phase of the gait cycle. Flat regions indicate when the feet are in contact with the floor (constant distance to the camera). As expected, it can also be seen that the Azure Kinect struggles when the distance is over 5 meters.

difference of 0.057 second from results obtained with a force plate when using 6 Azure Kinect cameras. This approach was used in this work for detecting HS's and TO's in this thesis thanks to its performance and ease of use.

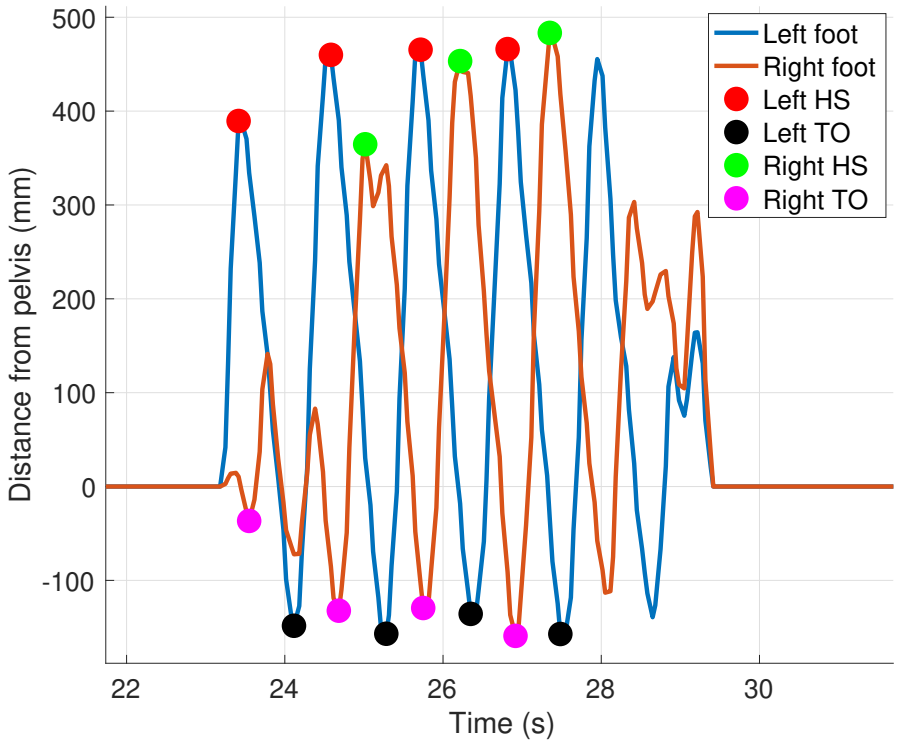

Figure 3.17: Plot of the feet position in relation to the pelvis and the detected HS's and TO's. The final footsteps were not counted because of the range limitations of the depth camera.

3.3 Discussion on Footstep Localization Trials

In addition to the discussion in Section 3.2, more observations are made here based on the results of the footstep localization experiment in GH.

3.3.1 Footstep Localization Accuracy

Although the vibration-based localization results in the x-direction were not reliable, they did not affect the results in the y-direction, thus allowing for the tracking of gait parameters in the direction of walking. The results also confirmed that the position estimates for footsteps

inside the convex-hull were more accurate than for those outside. Therefore, only footsteps that happened inside the convex-hull will be used to calculate spatial and temporal-spatial gait parameters. A simple solution for this limitation would be to position the start and end walking points inside the convex-hull.

It is also important to note that this algorithm requires a calibration phase to properly estimate the energy attenuation rate β. Using a fixed value for β has been proposed in [9], but the author mentions that this approach would almost always not yield the smallest possible localization MAE. It was shown in [12] that allowing β to vary during the nonlinear optimization solver will give the lowest error estimates, but finding the proper lower bound for β still needs to be done on-site because seismic waves travel differently depending on the floor system.

3.3.2 Localization Algorithm Computational Performance

The algorithms used in this study provided an adequate balance between accuracy and performance when compared to others described in Chapter 2. It took on average 0.07 second to obtain each footstep position estimate using the energy-based approach with a regular laptop without parallel computing, allowing this technique to be used in real-time footstep detection and position tracking. On the other hand, the Azure Kinect requires a powerful GPU to capture depth images, but detecting footsteps from them is fast and does not require a powerful computer if using the approach described in Section 3.2.4.

Chapter 4

Frailty Analysis via VBOI

Chapter 3 described the methods used to detect and localize footsteps using both the passive, vibration-based approach and using the Azure Kinect. This chapter presents gait analyzes results performed after the footstep detection and localization phases. To reiterate, walking trials were performed at both regular and fast walking speeds, and with and without added ankle weights for frailty simulation. For simplicity, let the walking trials without added weights be defined as "healthy gait trials (HGT)" and the ones with the added weights as "frail gait trials (FGT)". A total of 12 walking trails were conducted for each scenario, totaling 48 walking trials. Finally, paired two-sample t-tests for means were performed to compare results from both healthy and frail walking trials. The null hypothesis was that there would be no significant difference (p-value ≤ 0.05) between the different frailty groups.

4.1 Gait Speed

Three different methods were used to estimate gait speeds. Using the results from the vibration-based footstep localization algorithm, gait speeds for each walking trial were calculated as the average of the distance between consecutive steps divided by the difference in time. The Azure Kinect gait speed was calculated by dividing the distance traveled by the *Pelvis* joint in the z-direction by the total walking time. Gait speeds were also calculated by dividing the total walking distance by the walking time taken with a stopwatch, as it

is currently done in healthcare facilities. According to the literature, people suffering from frailty have significantly slower gait speed than healthy ones, therefore it was expected a decrease in gait speed during FGT [32, 47, 65].

Figure 4.1 shows the overall distributions of calculated gait speeds during the regular walking scenarios. It can be seen that the vibration approach was the least precise one but had small mean-absolute-differences (MD = $\frac{\sum_{k=1}^{N} ||\epsilon_k||}{N}$) relative to the Azure Kinect (0.49 m/s for healthy walks and 0.42 m/s for frail ones). The stopwatch method was more precise and had even smaller MD's of 0.07 m/s and 0.09 m/s during regular and fast walk trials, respectively. However, only the Kinect-based method provided enough evidence to reject the null hypothesis at usual walking speed as shown in Table 4.1.

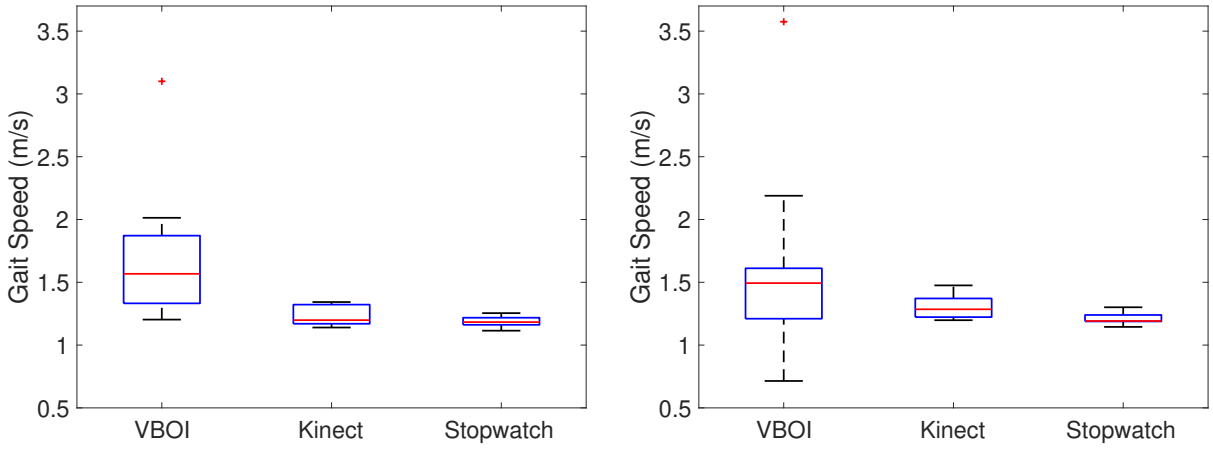

(a) Healthy walk. (b) Frail walk.

Figure 4.1: Gait speed distributions from walking trials at usual speed.

Since participants walk at different speeds, overall gait speed results can suffer from intra-participant variability. Thus, in order to obtain a fuller gait speed analysis, Figure 4.2 presents the results for each participant separately at usual gait speed. It can be seen that the vibration approach struggled the most to measure Participant 2's gait speed, probably because of light stepping and soft-soled shoes, which hinders the performance of the foot-

step detection algorithm as shown in Section 3.2. The vibration-based results also show that Participants 1 and 3 had similar mean gait speeds compared to the Kinect-based and stopwatch-based approaches, however, their range of calculated gait speeds was greater using the vibration approach. This is a consequence of the footstep localization algorithm performance which can be affected by different sources of variability such as walking speed, shoe type, and sensors position.

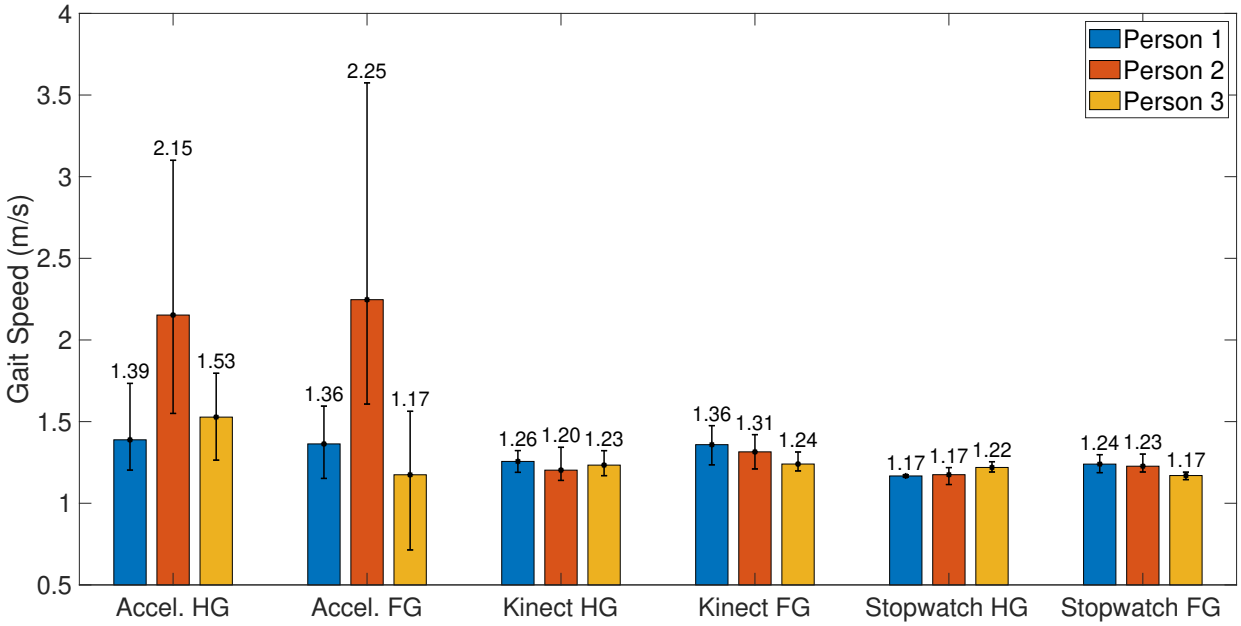

Figure 4.2: Plot of mean gait speed and gait speed ranges (black whiskers) for each participant. "HG" and "FG" stand for "healthy gait" and "frail gait", respectively.

Furthermore, almost all participants had faster mean gait speeds during FGT using the Kinect-based and stopwatch-based approaches, which goes against what is found in the literature as frailty should slow down gait speed. However, this could mean that the increased walking effort due to added weights inadvertently also increased the Participants' walking speed, especially when all participants were healthy and the added weights were only meant to simulate frailty. Given the participants' health and physical conditioning, it is possible that extra weight or other techniques were needed to better simulate a frailty status. Par-

ticipant 2 also had a higher mean gait speed during FGT using the vibration approach, but not Participants 1 and 3. Finally, given that the person using the stopwatch had to take 4 measurements per walking trial (as described in Section 3.1), it is possible that this person unconsciously took measurements based on a stopwatch clicking rhythm, rather than when the walking participant actually crosses specific checkpoints, which could explain the low variability within the stopwatch measurements.

At fast gait speeds, the difference between the three methods was smaller as shown in Figure 4.3. The vibration approach had an overall MD's of 0.38 m/s at HGT and 0.32 m/s during frail walking, while the stopwatch differences were 0.25 m/s and 0.17 m/s for both walking scenarios, respectively. By comparing Figure 4.3 to Figure 4.1 it can be seen that both the Kinect and the stopwatch methods had higher overall variability at fast walking trials and during trials at regular gait speed. On the other hand, the vibration results were less variable at fast walk when compared to results at usual walk and provided enough evidence to reject the null hypothesis.

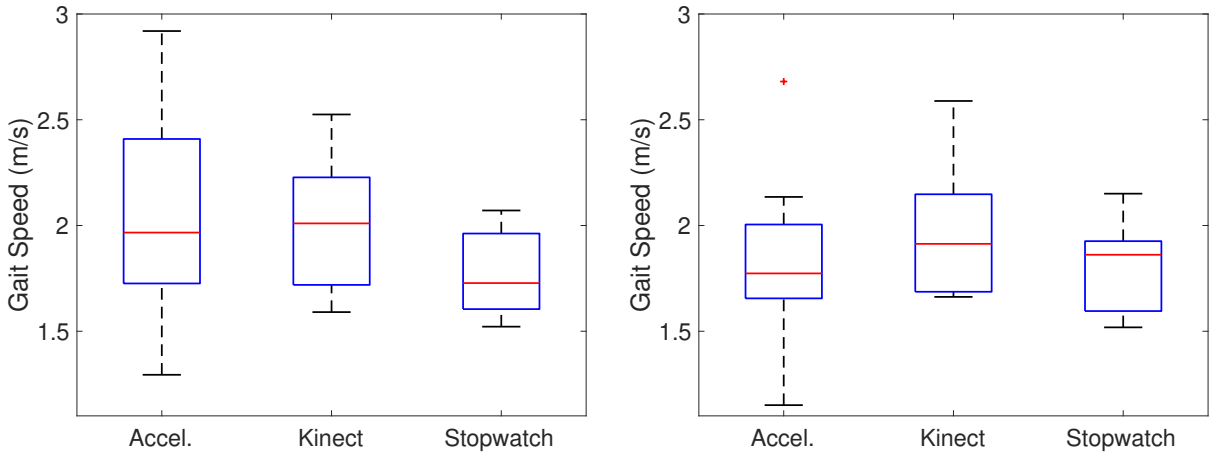

(a) Healthy walk.

(b) Frail walk.

Figure 4.3: Gait speed distributions from walking trials at fast speed.

Figure 4.4 shows the mean gait speeds for each participant during the fast walking trials.

Across all 3 measuring methods, Participant 1 had similar mean gait speeds between frailty groups, while Participant 3 had slower mean gait speeds between HGT and FGT. Participant 2 had a slower mean gait speed between HGT and FGT only via the vibration approach and had a smaller range gait speeds as well compared to walking at usual speed. The vibration approach had more similar results to both the Azure Kinect and the stopwatch at fast gait speeds than at regular speed. This is a result of the increased performance of the footstep localization algorithms as footsteps are easier to detect during fast walking.

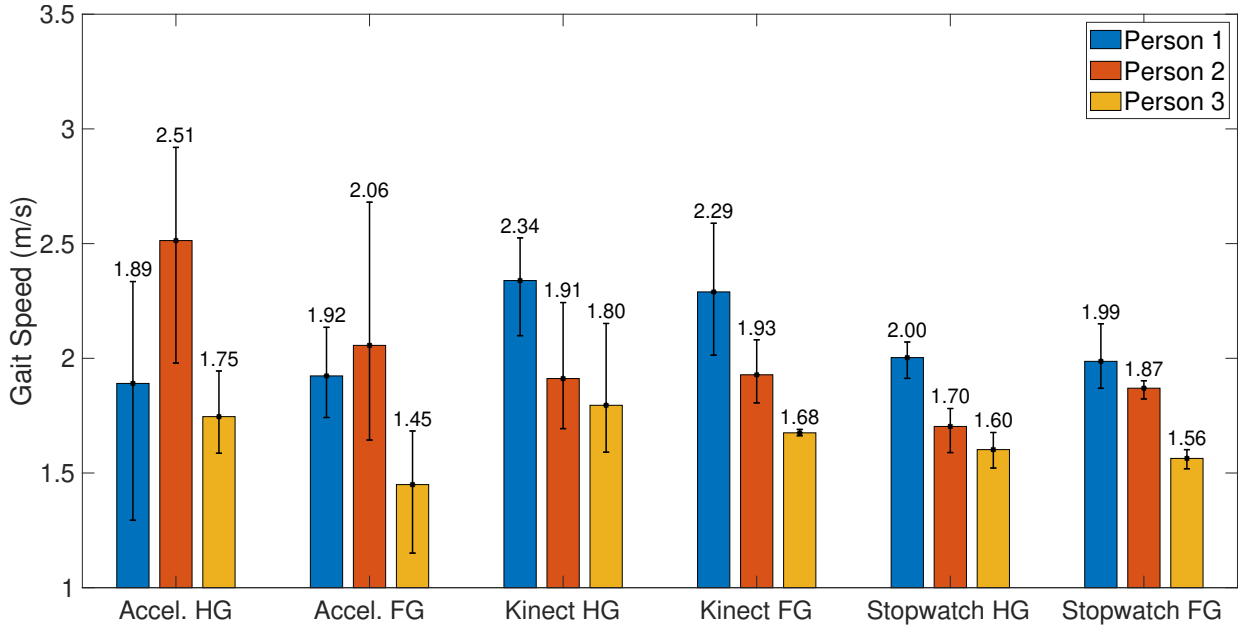

Figure 4.4: Plot of mean gait speed and gait speed ranges (black whiskers) for each participant at fast walking. "HG" and "FG" stand for "healthy gait" and "frail gait", respectively.

It is important to notice that although the vibration-based approach showed a significant difference at fast walking, the sample size was relatively small (only 12 trials), which could affect the power of the hypothesis test. When combined with the results from the other gait parameters, which will be discussed in the following sections, it is unlikely that only gait speed results would be significant when no other parameter was. Tests with a larger sample size are needed to increase the power of the hypothesis tests.

Lastly, Table 4.1 presents the summary statistics from gait speed results.

Table 4.1: Summary Statistics For Gait Speed Results.

	Usual Gait			Fast Gait		
	VBOI	Kinect	Stopwatch	VBOI	Kinect	Stopwatch
Healthy	1.69 ± 0.52^{a}	1.23 ± 0.08	1.19 ± 0.04	2.05 ± 0.47	2.02 ± 0.32	1.77 ± 0.19
Frail	1.59 ± 0.72	1.30 ± 0.10	1.21 ± 0.05	1.81 ± 0.40	1.96 ± 0.30	1.81 ± 0.20
Diff.[b]	-0.10	0.07	0.02	-0.24	-0.06	0.04
p-value	0.388	0.034*	0.230	0.050*	0.360	0.388

* - Significant ($p \leq 0.05$); [a] - Mean gait speed $\pm$ standard deviation in m/s;
[b] - Mean gait speed difference between frailty groups.

4.2 Cadence

Cadence was calculated according to Equation 4.1, but only with the vibration and Kinect methods as there were no simple ways to obtain it from stopwatch measurements. Just as with gait speed, a frail gait has usually a lower mean cadence than a healthy one [65, 66]. Results for walking at regular gait speed are shown in Figure 4.5 and at fast gait in Figure 4.6. Table 4.2 shows the summary statistics for walking trials at both speeds.

$$\text{Cadence} = \frac{\text{Number of Detected Footsteps}}{\text{Time Between } 1^{st} \text{ and last detected footstep (s)}} * \frac{60 \text{ s}}{\text{min}} \tag{4.1}$$

As mentioned previously, accelerometers are more effective for detecting when a vibration event happened than where it happened. Thus, as cadence does not depend on the footstep localization but only on footstep detection, the results from the vibration approach were more precise than the Kinect-based one. However, no overall significant differences were found for walking trials at both speeds, which could mean that the added weight did not significantly affect the participants' estimated cadence.

The MD values for walking trials at usual gait speed were 7.84 steps/min for healthy walks and 7.72 steps/min for frail walks. At fast gait the MD's increase to 20.41 steps/min and 17.96 steps/min at both HGT and FGT, respectively.

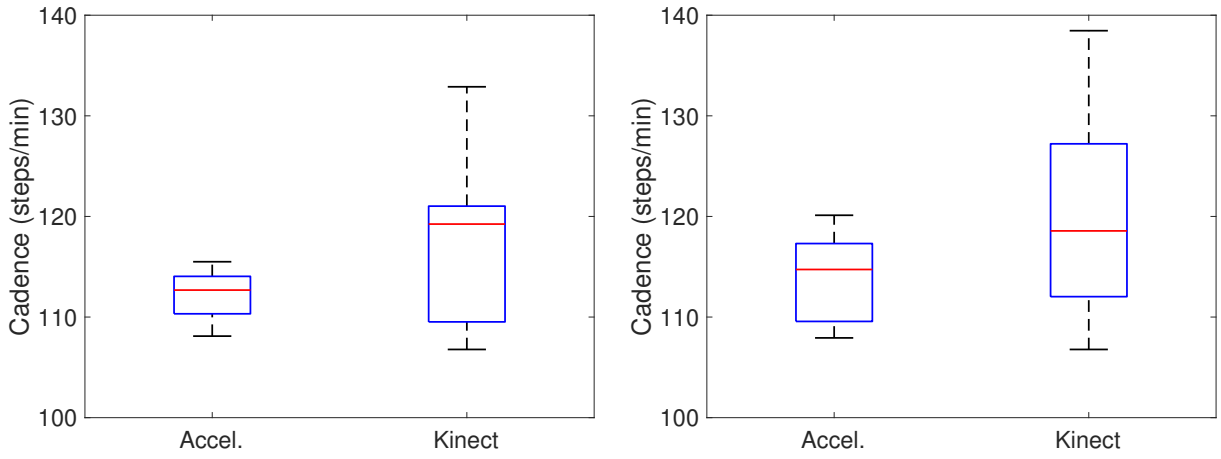

(a) Healthy walk. (b) Frail walk.

Figure 4.5: Cadence distributions from walking trials at usual walking speed.

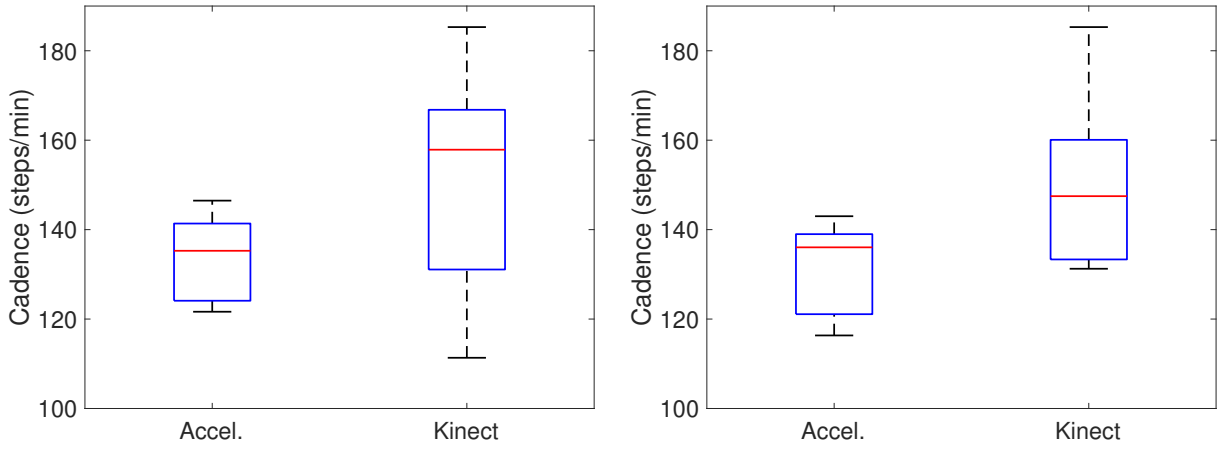

(a) Healthy walk. (b) Frail walk.

Figure 4.6: Cadence distributions from walking trials at fast walking speed.

One advantage of the vibration approach was detecting most footsteps throughout the entire

walk, while the Kinect could only accurately detect footsteps inside its depth camera range. Thus, as expected, the vibration approach was overall more effective at calculating cadence given its performance to detect heel strike events, particularly at fast walking speeds, in comparison to the Kinect.

Table 4.2: Summary Statistics For Cadence Results.

	Usual Gait		Fast Gait	
	VBOI	Kinect	VBOI	Kinect
Healthy	112.22 ± 2.42^a	117.37 ± 7.68	133.57 ± 9.17	150.75 ± 23.16
Frail	113.90 ± 4.22	120.16 ± 10.16	131.57 ± 9.91	149.53 ± 16.43
Diff.^{b}	1.68	2.79	-2.00	-1.22
p-value	0.299	0.378	0.190	0.743

^{a} - Mean cadence $\pm$ standard deviation in steps/min; ^{b} - Mean cadence difference between frailty groups.

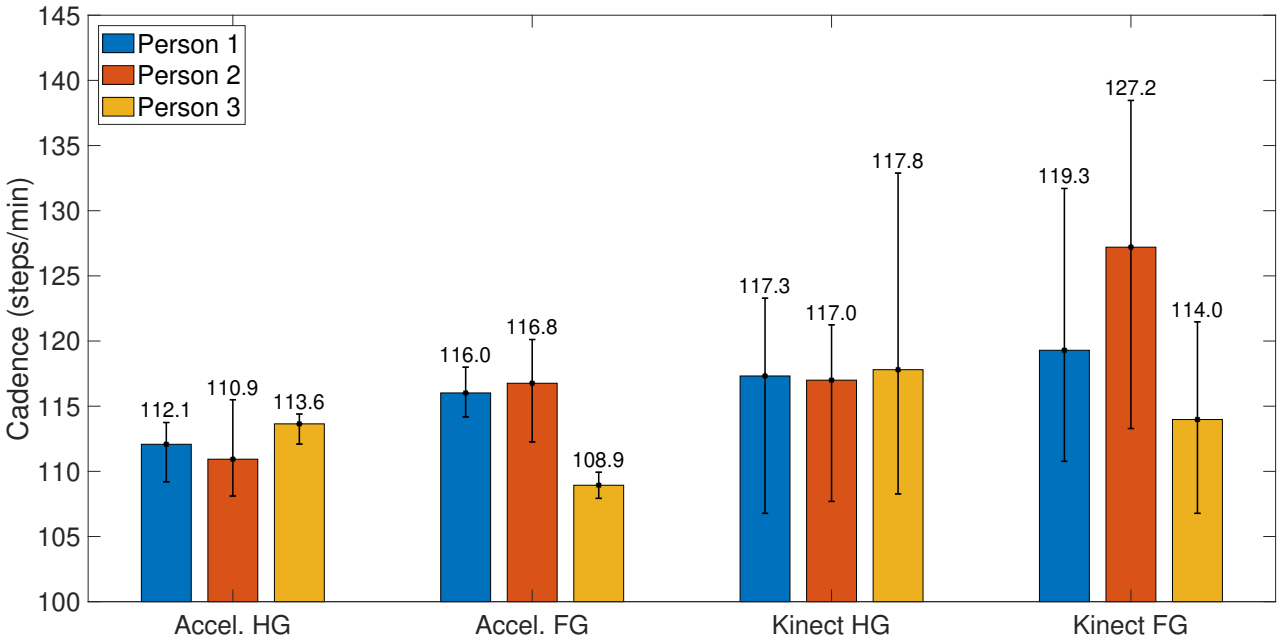

Figure 4.7: Mean cadence at usual gait for each participant with their corresponding cadence range (black whiskers).

Figures 4.7 and 4.8 show each participant's estimated cadence using both measuring methods. At usual walking, participants did not have large differences in mean cadence between frailty groups. A more observable difference can be seen during fast walking trials in which almost

every participant had a lower mean cadence between frailty groups. Results from the Kinect were significantly less precise than the ones from the accelerometers, therefore, the vibration-based approach is better at estimating cadence thanks to its capabilities of detecting temporal events.

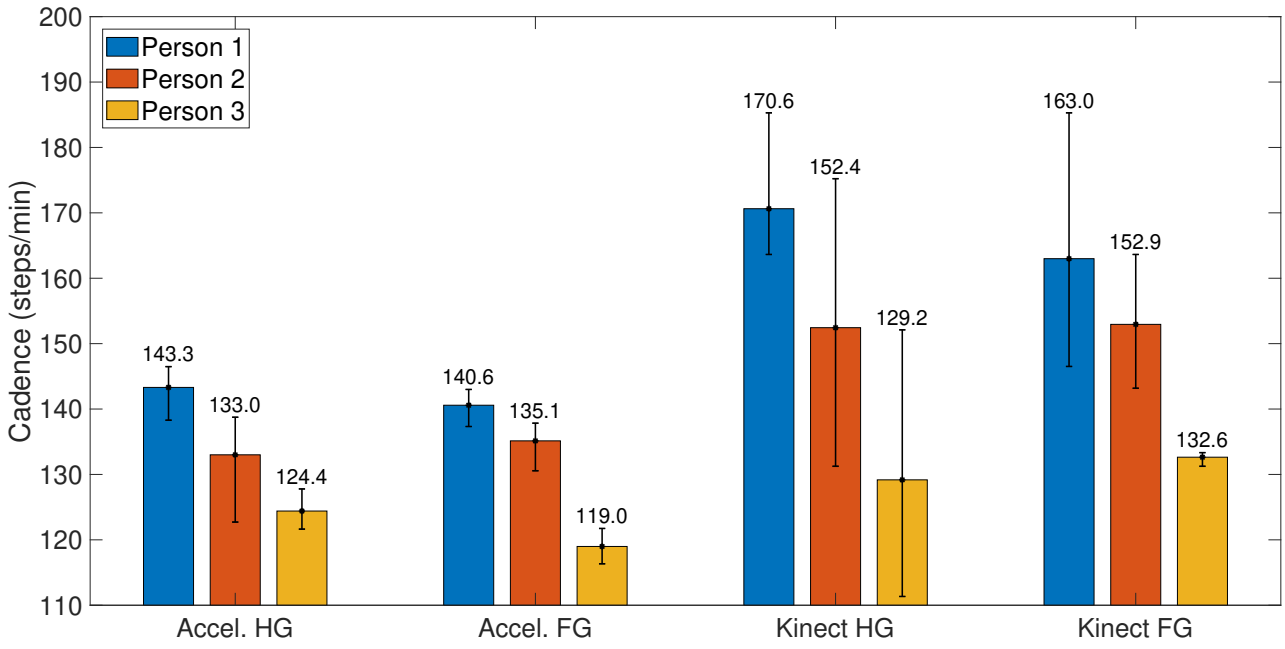

Figure 4.8: Mean cadence at fast gait for each participant with their corresponding cadence range (black whiskers).

4.3 Stride Variability

Stride length and time variability were also obtained from the vibration and Kinect methods. Stride variability is described by the coefficient of variation (CV) as shown in Equation 2.1. Low stride variability is linked to automatic and effortless walking, thus frail gait will most likely have higher variability than healthy ones [45, 65].

4.3.1 Stride Length

Stride length variability is a spatial gait parameter that measures distance changes between strides. It was calculated using the results from the vibration-based footstep localization algorithm and Kinect method. A range of stride length CV's from healthy to frail gait is around 2-10% according to previous research [65, 66], where the higher the variability, the worse the frailty status. Therefore, it can be seen from Figures 4.9 and 4.10 that the vibration-based algorithm was not able to accurately obtain the stride length variability, as the real stride lengths were unlikely to have varied more than 10%, especially during healthy walking trials.

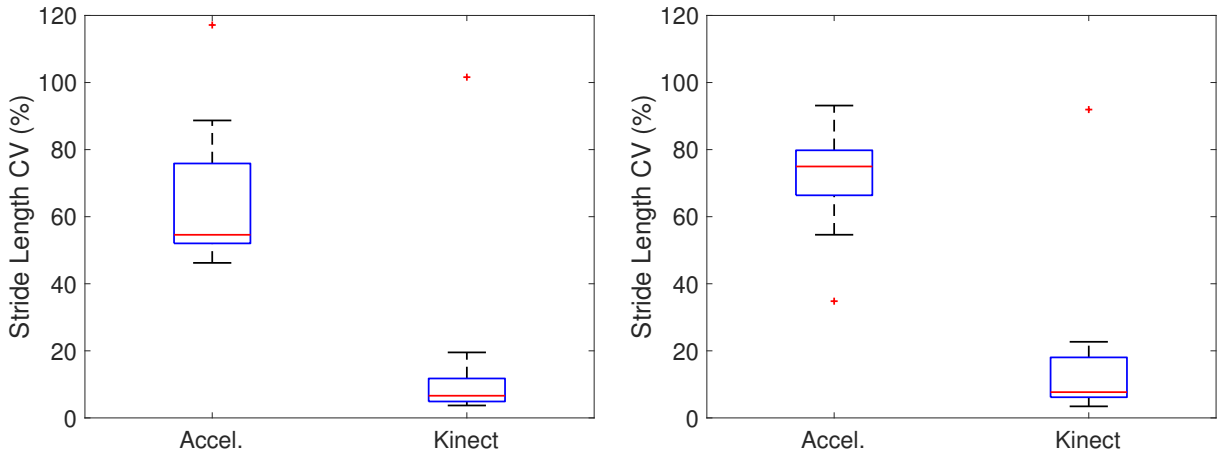

(a) Healthy walk. (b) Frail walk.

Figure 4.9: CV distributions from walking trials at usual walking speed.

The reason for such large CV values from the vibration approach is that, at its current state, the footstep-localization algorithm is not precise enough at localizing individual footsteps. Differently from gait speed, which also takes into account *when* a footstep happens, stride length depends exclusively on the spatial results of the vibration method. Although the algorithm is capable of, on average, performing to a sub-meter error (as shown in Section

3.2.3), individual estimations of the footsteps locations suffer from high variability, therefore affecting the stride length CV. Figure 3.10 is an example of the high variability of the energy-based algorithm, where the algorithm estimated the location of footstep number 7 to be lower than footsteps 8 and 9, meaning that the participant momentarily walked back towards the starting position when this did not actually happen. Such inconsistencies in the localization detection result in high CV's for stride lengths. However, an increase in stride variability during the frail walking trials can still be observed, particularly for usual walking. This could indicate that even though the mean CV was too large, the vibration approach is still capable of detecting an increase in stride length variability during FGT, but improvements to the localization algorithm are needed to obtain meaningful results.

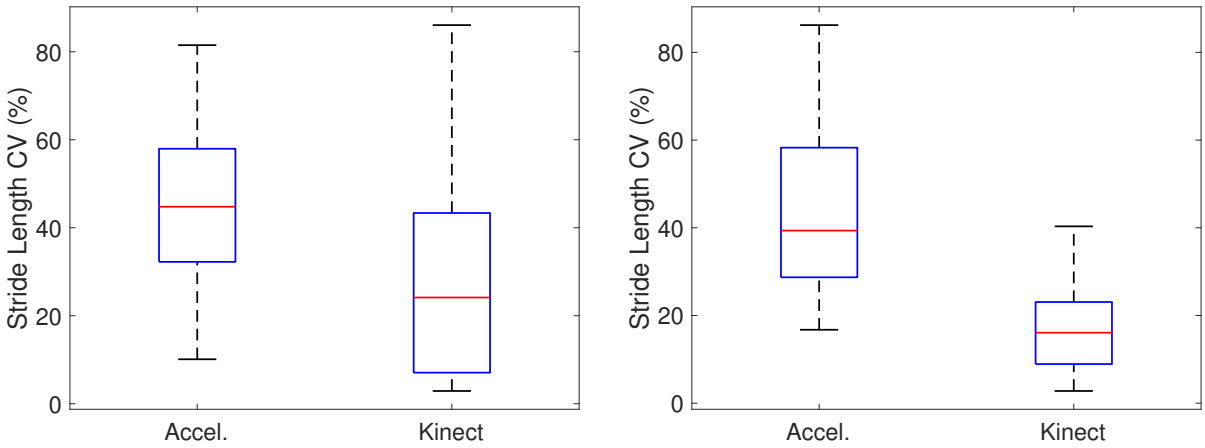

(a) Healthy walk.

(b) Frail walk.

Figure 4.10: CV distributions from walking trials at fast walking speed.

The Kinect performed better than the accelerometers, especially at regular walking speeds, but not by much. Its CV distributions were also larger than those described in the literature at both walking speeds and close to the vibration-based ones. This is again probably a result of only being able to track a few strides in each trial, especially at fast walking speed. The most interesting conclusions from the stride length variability are that both types of

sensors were not capable of accurately measuring it and that the vibration-based approach performed only slightly worse than the Kinect.

Finally, Table 4.3 describes the summary statistics for stride length variability, where no significant difference between frailty groups was observed in any walking scenario.

Table 4.3: Summary statistics for stride length variability results.

	Usual Gait		Fast Gait	
	VBOI	Kinect	VBOI	Kinect
Healthy	$65.28 \pm 21.15\%$[a]	$15.75 \pm 27.41\%$	$45.62 \pm 21.66\%$	$29.21 \pm 25.78\%$
Frail	$71.89 \pm 15.75\%$	$16.83 \pm 24.45\%$	$44.32 \pm 20.17\%$	$16.97 \pm 10.89\%$
Diff.[b]	6.61%	1.08%	−1.30%	−12.24%
p-value	0.409	0.920	0.863	0.156

[a] - Mean CV ± standard deviation; [b] - Mean stride length variability difference between frailty groups.

4.3.2 Stride Time Variability

Similar to cadence, stride time variability (also measured by the CV) only depends on the footstep detection in time, where accelerometers perform the best. It should come as no surprise that tracking stride time was better using accelerometers than the Kinect as the vibration CV results were compatible with those given in the literature and more precise. In fact, the opposite scenario to stride length variability (where the Kinect was slightly more precise) occurs with stride time variability. Figures 4.11 and 4.12 show the calculated stride time CV for each participant at both usual and fast walking trials, respectively. The vibration approach performed best during fast walking trials as it was more precise. An interesting observation is that stride time variability went down during FGT, indicating that the added ankle weight reduced stride variability instead of increasing it. As mentioned in Section 4.1, it is possible that the added weights did not simulate frailty well, thus the

reason for a reduction in stride time variability during FGT.

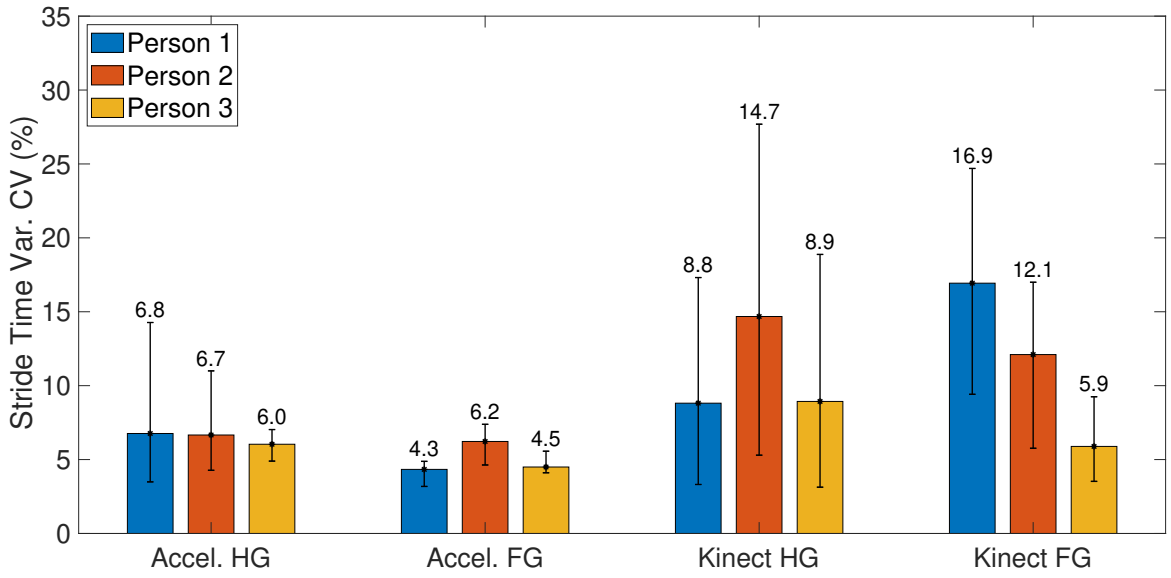

Figure 4.11: Mean stride time variability at usual gait for each participant with their corresponding CV's range (black whiskers).

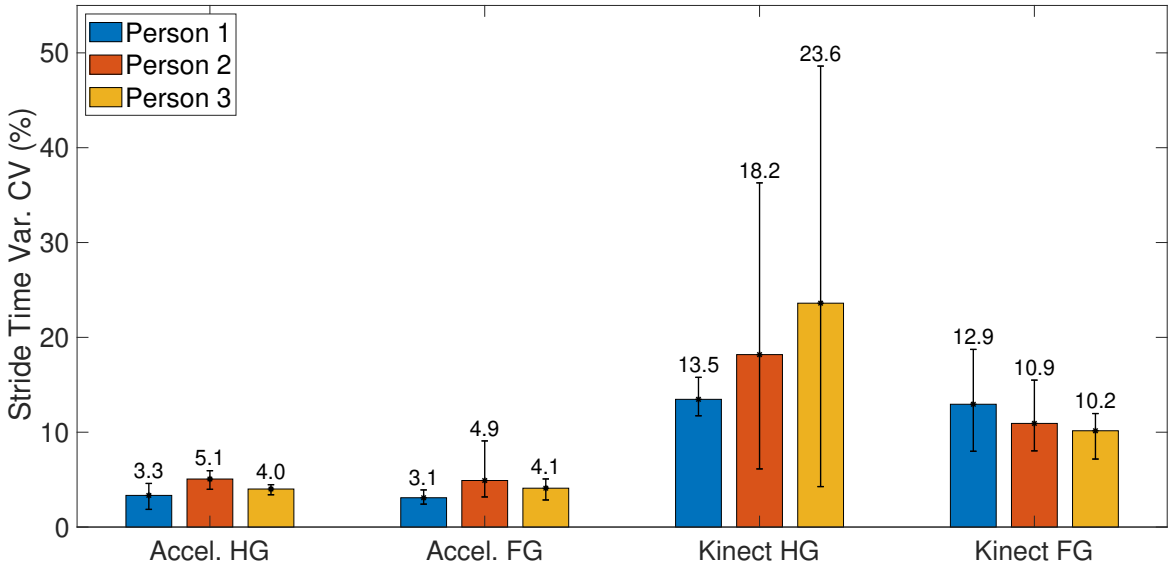

Figure 4.12: Mean stride time variability at fast gait for each participant with their corresponding CV's range (black whiskers).

Furthermore, it can be seen from Table 4.4 that there were no overall significant differences between frailty groups during any walking scenario.

Table 4.4: Summary statistics from stride time variability results.

	Usual Gait		Fast Gait	
	VBOI	Kinect	VBOI	Kinect
Not Frail	$6.49 \pm 3.13\%$[a]	$10.81 \pm 7.82\%$	$4.14 \pm 1.12\%$	$18.42 \pm 13.10\%$
Frail	$5.01 \pm 1.26\%$	$11.64 \pm 6.43\%$	$4.03 \pm 1.75\%$	$11.34 \pm 3.75\%$
Diff.[b]	-1.48%	0.83%	-0.11%	-7.08%
p-value	0.190	0.778	0.828	0.083

[a] - Mean CV $\pm$ standard deviation; [b] - Mean stride time variability difference between frailty groups.

4.4 Discussion

The results presented in this Chapter indicate that detecting frail gait parameters through current VBOI methods is possible to some extent. Temporal gait parameters were the easiest to track, followed by spatial-temporal ones. Thus, the vibration-based approach could be useful in real healthcare facilities considering that it was possible to track gait speed, the most important frailty predictor, within relatively small differences to the Kinect. The vibration approach also outperformed the Kinect when measuring gait cadence and stride time variability, while performing slightly worse than the Kinect when measuring stride length variability. The versatility of VBOI, combined with its passive nature and low patient privacy infringement, makes it an interesting alternative method for gait analysis in healthcare.

It is important, though, to address some of the limitations of the proposed VBOI system. Footstep localization is well-researched in VBOI and at its current state, such techniques are capable of sub-meter footstep localization and tracking of the direction of travel. However, more precision is needed in order to track spatial gait variations in frailty diagnosis. Increased performance of the localization algorithm would be beneficial in estimating gait speed, for example. In fact, Figure 4.13 provides an interesting example of what would happen if the

temporal parameter of footsteps (when they happened, measured with accelerometers) was combined with the average step length (measured with the Kinect) to calculate gait speed. The results are more precise (with MD from the Kinect of 0.19 m/s) than only using VBOI alone.

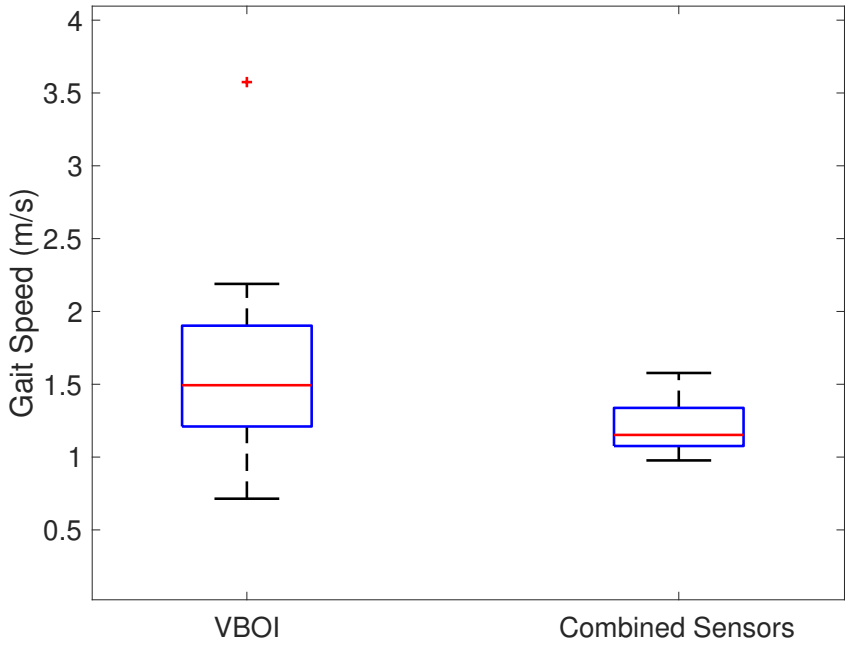

Figure 4.13: Gait speed results from using VBOI alone and the gait speed obtained from using improved step length from the Kinect combined with temporal information from the accelerometers.

As described in Chapter 3, conducting trials at a fast walking speed positively affects the detection of footsteps. Given that the vibration-based footstep detection and localization algorithm performed better at fast walking, combined with the fact that patients tend to show clearer signs of underlying health issues when walking at a faster pace [45], makes conducting clinical trials at a fast gait speed more beneficial when using VBOI.

The number of accelerometers used and their mounting position also affect the footstep localization accuracy. In tracking spatial gait parameters, the localization accuracy tends

to increase as the number of sensors increases [11]. That is why most of the energy-based footstep detection and localization algorithms researched in GH used more than 10 underfloor accelerometers, distributed not only at the boundaries of the hallway but also directly in the middle of it [9, 10, 11, 38]. Therefore, increasing the sensor density could improve the footstep localization performance and increase the precision in stride time variability.

Nevertheless, as shown in this Chapter, VBOI can provide a new and exciting method of gait frailty analysis that is non-intrusive, fast, and does not affect patient privacy as long as its limitations are taken into consideration.

Chapter 5

Conclusions

This thesis will conclude by summarizing the contributions of this work and discuss future improvements in frailty gait analysis via VBOI.

5.1 Thesis Summary

In Chapter 2 a review of current frailty definitions and diagnosis techniques has been provided. It was demonstrated that although frailty is an important public health issue, diagnosing it early is a difficult task in healthcare. However, gait parameters such as gait speed, are strong indicators of a patient's frailty status, and different methods of tracking them have been proposed in the literature. In addition to a review of human frailty, Chapter 2 also provided a review of current VBOI techniques and their proposed advantages in gait analysis that could aid healthcare providers in frailty diagnosis.

Chapter 3 provided an in-depth look at the vibration-based footstep detection and localization techniques used in this work, as well as the algorithms used with the Azure Kinect. It was shown that footstep detection was easier for participants walking at fast gait speed and not wearing soft-sole shoes. The localization algorithm had sub-meter overall accuracy for footsteps inside the sensors convex-hull. The Azure Kinect performed better at regular walking speeds trials because of its limited sensor range and the number of cameras used.

In Chapter 4 the results from frailty diagnosis via VBOI were presented. The vibration-based approach obtained comparable gait speed results to the Kinect, especially at fast gait trials. It was also more precise in measuring cadence and stride time variability. The only parameter that the vibration approach did not perform well was stride length variability, where results were highly affected by the different sources of uncertainties in the VBOI method, but were close to results from the Kinect. Finally, a discussion on the gait analysis results and possible algorithm improvements was provided.

5.2 Deployment Considerations

Based on the results from this work, there are a few recommendations for deploying and using the VBOI method for frail gait analysis in the field. These include:

- **Sensor Position and Density** - It is beneficial to place sensors in a calm region, with as few sources of vibration noise as possible, e.g., constant opening and closing of doors, people walking, or machine running. It is important to place sensors as far away as possible from structural walls to avoid wave distortions and reflections as was experienced during this work. Increasing the sensor density could also increase the accuracy of the detection and localization algorithm.

- **Walking Path** - The total walking area should be enclosed by the convex-hull of the sensors so that every footstep can be properly localized and used in the gait parameter calculations.

- **Walking Speed** - As discussed previously in Chapter 4, there are multiple benefits from conducting trials at a fast gait speed. However, this walking scenario might introduce safety concerns, particularly if the participants are suffering from severe

frailty, therefore the test conductor must carefully evaluate all safety factors before running trials at fast gait speeds.

5.3 Future Work in VBOI Gait Analysis

The contribution in Chapter 4 demonstrated that VBOI gait analysis provides promising new techniques for gait parameters measurement in healthcare. However, an increased footstep localization precision is needed so that VBOI could be fully utilized in frailty analysis. This could be reached if VBOI techniques also took into consideration a more detailed understanding of the fundamental dynamics of structural buildings, which would reduce the number of assumptions made, and ensure that these techniques could be universally applied in different structures. Such a limitation was experienced during this work as the placing of floor-mounted accelerometers affected the localization results, by limiting the algorithm performance in localizing footsteps in the x-direction of the hallway (along its width). Therefore, acquiring more information about the structure, as it is done with data and model-driven techniques [25], could help improve the footstep localization accuracy. As discussed in [39], VBOI has currently benefited from individual works where some occupant inference parameter is measured and validated within one testing scenario and utilizing specific floor dynamics assumptions (such as infinite plate or no wave reflections). This results in the development of individual algorithms that have different floor dynamics assumptions and little overlap. Perhaps VBOI would benefit better from algorithms that are more integrated with each other thus having a more robust understanding of the vibration dynamics in the testing area.

Lastly, the author believes that VBOI research is still too focused on the development of algorithms and their validation with experimental data from controlled settings, rather than

their deployment and applications in real-world scenarios. For example, most footstep localization algorithms described in Chapters 2 and 3 have been thoroughly tested in optimal conditions, where there is usually only one person walking at a time and there are little building activities (other people walking or doors closing) that could introduce vibration noise in their measurements, and using specific accelerometers at specific spots. However, there is no guarantee that those conditions will be met outside the lab. Hospitals, for example, are usually busy places where there are constant sources of human, equipment, and object-induced vibrations, so if vibration-based gait analysis is to be applied in healthcare, there is the need for a greater understanding of how VBOI techniques perform outside the lab. Studying the limitations of VBOI, and where it fails, would provide not only new research opportunities, but also a greater understanding of exactly where and how these techniques can be applied.

Bibliography

[1] Apple iphone xs. http://www.apple.com/. Accessed: 2020-02-15.

[2] GAITRite world leader in temporospatial gait analysis. https://www.gaitrite.com/. Accessed: 2020-02-15.

[3] MATLAB math. graphics. programming. https://www.mathworks.com/products/matlab.html. Accessed: 2020-02-15.

[4] Azure Kinect azure kinect dk – develop ai models: Microsoft azure. https://azure.microsoft.com/en-us/services/kinect-dk/. Accessed: 2020-02-15.

[5] Vicon award winning motion capture systems. https://www.vicon.com/. Accessed: 2020-02-15.

[6] PcB Piezotronics sensors to measure vibration, acoustics, force, pressure, load, strain, shock & torque. https://www.pcb.com/. Accessed: 2020-02-15.

[7] Ivo L. Abraham, Carol A. Manning, Mary R. Boyd, Jane B. Neese, Maureen C. Newman, Lisa Ann Plowfield, and Sally J. Reel. Cognitive screening of nursing home residents: Factor structure of the modified mini-mental state (3ms) examination. *International Journal of Geriatric Psychiatry*, 8(2):133–138, Feb 1993. ISSN 0885-6230, 1099-1166. doi: 10.1002/gps.930080205.

[8] Jonathan Afilalo. Frailty in patients with cardiovascular disease: Why, when, and how to measure. *Current Cardiovascular Risk Reports*, 5(5):467, 2011.

[9] Sa'ed Alajlouni and Pablo Tarazaga. A new fast and calibration-free method for footstep impact localization in an instrumented floor. *Journal of Vibration and Control*, 25(10):

1629–1638, 2019. doi: 10.1177/1077546319829943. URL https://doi.org/10.1177/1077546319829943.

[10] Sa'ed Alajlouni and Pablo Tarazaga. A passive energy-based method for footstep impact localization, using an underfloor accelerometer sensor network with kalman filtering. *Journal of Vibration and Control*, 26(11–12):941–951, Jun 2020. ISSN 1077-5463, 1741-2986. doi: 10.1177/1077546319890520.

[11] Sa'ed Alajlouni, Mohammad Albakri, and Pablo Tarazaga. Impact localization in dispersive waveguides based on energy-attenuation of waves with the traveled distance. *Mechanical Systems and Signal Processing*, 105:361–376, 2018. ISSN 0888-3270. doi: https://doi.org/10.1016/j.ymssp.2017.12.007. URL https://www.sciencedirect.com/science/article/pii/S0888327017306428.

[12] Justin Amadeus Albert, Victor Owolabi, Arnd Gebel, Clemens Markus Brahms, Urs Granacher, and Bert Arnrich. Evaluation of the pose tracking performance of the azure kinect and kinect v2 for gait analysis in comparison with a gold standard: A pilot study. *Sensors*, 20(18):5104, 2020.

[13] K. Aminian, B. Najafi, C. Büla, P.F. Leyvraz, and P. Robert. Spatio-temporal parameters of gait measured by an ambulatory system using miniature gyroscopes. *Journal of Biomechanics*, 35(5):689–699, May 2002. ISSN 00219290. doi: 10.1016/S0021-9290(02)00008-8.

[14] R. Bahroun, Olivier Michel, François Frassati, Mikael Carmona, and Jean-Louis Lacoume. New algorithm for footstep localization using seismic sensors in an indoor environment. *Journal of Sound and Vibration*, 333(3):1046–1066, 2014.

[15] Dustin Bales, Pablo A. Tarazaga, Mary Kasarda, Dhruv Batra, A. G. Woolard, J. D. Poston, and V. V. N. S Malladi. Gender classification of walkers via underfloor ac-

celerometer measurements. *IEEE Internet of Things Journal*, 3(6):1259–1266, Dec 2016. ISSN 2327-4662. doi: 10.1109/JIOT.2016.2582723.

[16] Flavio Bertini, Giacomo Bergami, Danilo Montesi, Giacomo Veronese, Giulio Marchesini, and Paolo Pandolfi. Predicting frailty condition in elderly using multidimensional socioclinical databases. *Proceedings of the IEEE*, 106(4):723–737, 2018. doi: 10.1109/JPROC.2018.2791463.

[17] Jennifer S. Brach, Stephanie A. Studenski, Subashan Perera, Jessie M. VanSwearingen, and Anne B. Newman. Gait variability and the risk of incident mobility disability in community-dwelling older adults. *The Journals of Gerontology Series A: Biological Sciences and Medical Sciences*, 62(9):983–988, 2007.

[18] J. C. Brown, M. O. Harhay, and M. N. Harhay. Physical function as a prognostic biomarker among cancer survivors. *British Journal of Cancer*, 112(1):194–198, Jan 2015. ISSN 0007-0920, 1532-1827. doi: 10.1038/bjc.2014.568.

[19] Yiu-Tong Chan and K.C. Ho. A simple and efficient estimator for hyperbolic location. *IEEE Transactions on Signal Processing*, 42(8):1905–1915, 1994.

[20] Joe C. Chen, Kung Yao, and Ralph E. Hudson. Source localization and beamforming. *IEEE Signal Processing Magazine*, 19(2):30–39, 2002.

[21] Joe C. Chen, Kung Yao, Tai-Lai Tung, Chris W. Reed, and Daching Chen. Source localization and tracking of a wideband source using a randomly distributed beamforming sensor array. *The International Journal of High Performance Computing Applications*, 16(3):259–272, 2002.

[22] Francesco Ciampa and Michele Meo. Acoustic emission source localization and velocity

determination of the fundamental mode a0 using wavelet analysis and a newton-based optimization technique. *Smart Materials and Structures*, 19(4):427, 2010.

[23] Yeates Conwell, Nicholas T. Forbes, Christopher Cox, and Eric D. Caine. Validation of a measure of physical illness burden at autopsy: The cumulative illness rating scale. *Journal of the American Geriatrics Society*, 41(1):38–41, Jan 1993. ISSN 00028614. doi: 10.1111/j.1532-5415.1993.tb05945.x.

[24] Silvia Lanziotti Azevedo da Silva, Joana Ude Viana, Vanessa Gomes Da Silva, João Marcos Domingues Dias, Leani Sousa Máximo Pereira, and Rosangela Correa Dias. Influence of frailty and falls on functional capacity and gait in community-dwelling elderly individuals. *Topics in Geriatric Rehabilitation*, 28(2):128–134, 2012.

[25] Benjamin T. Davis, Juan M. Caicedo, and Victor A. Hirth. Force estimation and event localization (feel) of impacts using structural vibrations. *Journal of Engineering Mechanics*, 147(3):201, 2021.

[26] Slah Drira, Yves Reuland, Sai G.S. Pai, Hae Young Noh, and Ian F.C. Smith. Model-based occupant tracking using slab-vibration measurements. *Frontiers in Built Environment*, 5:63, 2019.

[27] Kristine E. Ensrud, Susan K. Ewing, Brent C. Taylor, Howard A. Fink, Peggy M. Cawthon, Katie L. Stone, Teresa A. Hillier, Jane A. Cauley, Marc C. Hochberg, Nicolas Rodondi, J. Kathleen Tracy, Steven R. Cummings, and Study of Osteoporotic Fractures Research Group. Comparison of 2 Frailty Indexes for Prediction of Falls, Disability, Fractures, and Death in Older Women. *Archives of Internal Medicine*, 168(4):382–389, 02 2008. ISSN 0003-9926. doi: 10.1001/archinternmed.2007.113. URL https://doi.org/10.1001/archinternmed.2007.113.

[28] N. Seyma Erdem, Cem Ersoy, and Can Tunca. Gait analysis using smartwatches. In *2019 IEEE 30th International Symposium on Personal, Indoor and Mobile Radio Communications (PIMRC Workshops)*, pages 1–6. IEEE, 2019.

[29] Konrad Fassbender, Robin L. Fainsinger, Mary Carson, and Barry A. Finegan. Cost trajectories at the end of life: The canadian experience. *Journal of Pain and Symptom Management*, 38(1):75–80, Jul 2009. ISSN 08853924. doi: 10.1016/j.jpainsymman.2009.04.007.

[30] Xavier Ferre, Elena Villalba-Mora, Maria-Angeles Caballero-Mora, Alberto Sanchez, Williams Aguilera, Nuria Garcia-Grossocordon, Laura Nuñez-Jimenez, Leocadio Rodríguez-Mañas, Qin Liu, and Francisco del Pozo-Guerrero. Gait speed measurement for elderly patients with risk of frailty. *Mobile Information Systems*, 2017:1–11, 2017. ISSN 1574-017X, 1875-905X. doi: 10.1155/2017/1310345.

[31] Renato Campos Freire Junior, Jaqueline Mello Porto, Natália Camargo Rodrigues, Roberta de Matos Brunelli, Luis Felipe Pinto Braga, and Daniela Cristina Carvalho de Abreu. Spatial and temporal gait characteristics in pre-frail community-dwelling older adults. *Geriatrics & Gerontology International*, 16(10):1102–1108, 2016. doi: https://doi.org/10.1111/ggi.12594. URL https://onlinelibrary.wiley.com/doi/abs/10.1111/ggi.12594.

[32] L. P. Fried, C. M. Tangen, J. Walston, A. B. Newman, C. Hirsch, J. Gottdiener, T. Seeman, R. Tracy, W. J. Kop, G. Burke, and et al. Frailty in older adults: Evidence for a phenotype. *The Journals of Gerontology Series A: Biological Sciences and Medical Sciences*, 56(3):M146–M157, Mar 2001. ISSN 1079-5006, 1758-535X. doi: 10.1093/gerona/56.3.M146.

[33] Alan Godfrey, Silvia Del Din, Gillian Barry, J.C. Mathers, and Lynn Rochester. In-

strumenting gait with an accelerometer: a system and algorithm examination. *Medical Engineering & Physics*, 37(4):400–407, 2015.

[34] Jeffrey M. Hausdorff. Gait variability: Methods, modeling and meaning. *Journal of Neuroengineering and Rehabilitation*, 2(1):1–9, 2005.

[35] Delaram Jarchi, James Pope, Tracey K. M. Lee, Larisa Tamjidi, Amirhosein Mirzaei, and Saeid Sanei. A review on accelerometry-based gait analysis and emerging clinical applications. *IEEE Reviews in Biomedical Engineering*, 11:177–194, 2018. ISSN 1937-3333, 1941-1189. doi: 10.1109/RBME.2018.2807182.

[36] David M. Jones, Xiaowei Song, and Kenneth Rockwood. Operationalizing a frailty index from a standardized comprehensive geriatric assessment. *Journal of the American Geriatrics Society*, 52(11):1929–1933, 2004. doi: https://doi.org/10.1111/j.1532-5415.2004.52521.x. URL https://agsjournals.onlinelibrary.wiley.com/doi/abs/10.1111/j.1532-5415.2004.52521.x.

[37] M. Kasarda, P. Tarazaga, M. Embree, S. Gugercin, A. Woolard, B. Joyce, and J. Hamilton. Detection and identification of firearms upon discharge using floor-based accelerometers. In *Special Topics in Structural Dynamics, Volume 6*, pages 45–53. Springer, 2016.

[38] Ellis Kessler, Vijaya V.N. Sriram Malladi, and Pablo A. Tarazaga. Vibration-based gait analysis via instrumented buildings. *International Journal of Distributed Sensor Networks*, 15(10):1550147719881608, 2019.

[39] Ellis C. Kessler. *A Physically Informed Data-Driven Approach to Analyze Human Induced Vibration in Civil Structures*. PhD thesis, Virginia Tech, 2021.

[40] Christine E. King and Majid Sarrafzadeh. A survey of smartwatches in remote health monitoring. *Journal of Healthcare Informatics Research*, 2(1):1–24, 2018.

[41] Reto W. Kressig, Robert J. Gregor, Alanna Oliver, Dwight Waddell, Webb Smith, Michael O'Grady, Aaron T. Curns, Michael Kutner, and Steven L. Wolf. Temporal and spatial features of gait in older adults transitioning to frailty. *Gait & Posture*, 20(1): 30–35, 2004.

[42] Bing Liu, Xinhua Hu, Qiang Zhang, Yichuan Fan, Jun Li, Rui Zou, Ming Zhang, Xiuqi Wang, and Junpeng Wang. Usual walking speed and all-cause mortality risk in older people: A systematic review and meta-analysis. *Gait & Posture*, 44:172–177, 2016. ISSN 0966-6362. doi: https://doi.org/10.1016/j.gaitpost.2015.12.008. URL https://www.sciencedirect.com/science/article/pii/S0966636215009765.

[43] Andrew L. McDonough, Mitchell Batavia, Fang C. Chen, Soonjung Kwon, and James Ziai. The validity and reliability of the gaitrite system's measurements: A preliminary evaluation. *Archives of Physical Medicine and Rehabilitation*, 82(3):419–425, 2001.

[44] H. B. Menz. Age-related differences in walking stability. *Age and Ageing*, 32(2):137–142, Mar 2003. ISSN 00020729, 14682834. doi: 10.1093/ageing/32.2.137.

[45] M. Montero-Odasso, S. W. Muir, M. Hall, T. J. Doherty, M. Kloseck, O. Beauchet, and M. Speechley. Gait variability is associated with frailty in community-dwelling older adults. *The Journals of Gerontology Series A: Biological Sciences and Medical Sciences*, 66A(5):568–576, May 2011. ISSN 1079-5006, 1758-535X. doi: 10.1093/gerona/glr007.

[46] Jeretta Horn Nord, Alex Koohang, and Joanna Paliszkiewicz. The internet of things: Review and theoretical framework. *Expert Systems with Applications*, 133:97–108, 2019.

[47] Frederic Pamoukdjian, Elena Paillaud, Laurent Zelek, Marie Laurent, Vincent Lévy, Thierry Landre, and Georges Sebbane. Measurement of gait speed in older adults to identify complications associated with frailty: A systematic review. *Journal of Geriatric Oncology*, 6(6):484–496, Nov 2015. ISSN 18794068. doi: 10.1016/j.jgo.2015.08.006.

[48] Shijia Pan, Amelie Bonde, Jie Jing, Lin Zhang, Pei Zhang, and Hae Young Noh. Boes: Building occupancy estimation system using sparse ambient vibration monitoring. In *Sensors and Smart Structures Technologies for Civil, Mechanical, and Aerospace Systems 2014*, volume 9061, page 96O. International Society for Optics and Photonics, 2014.

[49] Neal Patwari, Alfred O. Hero, Matt Perkins, Neiyer S. Correal, and Robert J. O'dea. Relative location estimation in wireless sensor networks. *IEEE Transactions on Signal Processing*, 51(8):2137–2148, 2003.

[50] Jeffrey D. Poston, Javier Schloemann, R. Michael Buehrer, V.V.N. Sriram Malladi, Americo G. Woolard, and Pablo A. Tarazaga. Towards indoor localization of pedestrians via smart building vibration sensing. In *2015 International Conference on Localization and GNSS (ICL-GNSS)*, pages 1–6. IEEE, 2015.

[51] Jeffrey D. Poston, R. Michael Buehrer, Americo G. Woolard, and Pablo A. Tarazaga. Indoor positioning from vibration localization in smart buildings. In *2016 IEEE/ION Position, Location and Navigation Symposium (PLANS)*, pages 366–372. IEEE, 2016.

[52] M.T.E. Puts, P. Lips, and D.J.H. Deeg. Static and dynamic measures of frailty predicted decline in performance-based and self-reported physical functioning. *Journal of Clinical Epidemiology*, 58(11):1188–1198, 2005. ISSN 0895-4356. doi: https://doi.org/10.1016/j.jclinepi.2005.03.008. URL https://www.sciencedirect.com/science/article/pii/S0895435605001496.

[53] V. Racic, A. Pavic, and J.M.W. Brownjohn. Experimental identification and analytical modelling of human walking forces: Literature review. *Journal of Sound and Vibration*, 326(1):1–49, 2009. ISSN 0022-460X. doi: https://doi.org/10.1016/j.jsv.2009.04.020. URL https://www.sciencedirect.com/science/article/pii/S0022460X09003381.

[54] Giovanni Ravaglia, Paola Forti, Anna Lucicesare, Nicoletta Pisacane, Elisa Rietti, and Christopher Patterson. Development of an Easy Prognostic Score for Frailty Outcomes in the Aged. *Age and Ageing*, 37(2):161–166, 01 2008. ISSN 0002-0729. doi: 10.1093/ageing/afm195. URL https://doi.org/10.1093/ageing/afm195.

[55] Thomas N. Robinson, Jeffrey I. Wallace, Daniel S. Wu, Arek Wiktor, Lauren F. Pointer, Shirley M. Pfister, Terra J. Sharp, Mary J. Buckley, and Marc Moss. Accumulated frailty characteristics predict postoperative discharge institutionalization in the geriatric patient. *Journal of the American College of Surgeons*, 213(1):37–42, Jul 2011. ISSN 10727515. doi: 10.1016/j.jamcollsurg.2011.01.056.

[56] Thomas N. Robinson, Daniel S. Wu, Gregory V. Stiegmann, and Marc Moss. Frailty predicts increased hospital and six-month healthcare cost following colorectal surgery in older adults. *The American Journal of Surgery*, 202(5):511–514, Nov 2011. ISSN 00029610. doi: 10.1016/j.amjsurg.2011.06.017.

[57] K. Rockwood, Xiaowei Song, Chris MacKnight, Howard Bergman, David B. Hogan, Ian McDowell, and Arnold Mitnitski. A global clinical measure of fitness and frailty in elderly people. *Canadian Medical Association Journal*, 173(5):489–495, Aug 2005. ISSN 0820-3946, 1488-2329. doi: 10.1503/cmaj.050051.

[58] Kenneth Rockwood. Frailty and its definition: A worthy challenge. *Journal of the American Geriatrics Society*, 53(6):1069–1070, Jun 2005. ISSN 00028614, 15325415. doi: 10.1111/j.1532-5415.2005.53312.x.

[59] Kenneth Rockwood, Karen Stadnyk, Chris MacKnight, Ian McDowell, Réjean Hébert, and David B Hogan. A brief clinical instrument to classify frailty in elderly people. *The Lancet*, 353(9148):205–206, Jan 1999. ISSN 01406736. doi: 10.1016/S0140-6736(98)04402-X.

[60] Leocadio Rodríguez-Mañas, Catherine Féart, Giovanni Mann, Jose Viña, Somnath Chatterji, Wojtek Chodzko-Zajko, Magali Gonzalez-Colaço Harmand, Howard Bergman, Laure Carcaillon, Caroline Nicholson, and et al. Searching for an operational definition of frailty: A delphi method based consensus statement. the frailty operative definition-consensus conference project. *The Journals of Gerontology: Series A*, 68(1): 62–67, Jan 2013. ISSN 1758-535X, 1079-5006. doi: 10.1093/gerona/gls119.

[61] Darryl B. Rolfson, Sumit R. Majumdar, Ross T. Tsuyuki, Adeel Tahir, and Kenneth Rockwood. Validity and Reliability of the Edmonton Frail Scale. *Age and Ageing*, 35(5):526–529, 06 2006. ISSN 0002-0729. doi: 10.1093/ageing/afl041. URL https://doi.org/10.1093/ageing/afl041.

[62] Marc D. Rothman, Linda Leo-Summers, and Thomas M. Gill. Prognostic significance of potential frailty criteria. *Journal of the American Geriatrics Society*, 56(12):2211–2216, Dec 2008. ISSN 00028614, 15325415. doi: 10.1111/j.1532-5415.2008.02008.x.

[63] Rodrigo Sarlo and Pablo A. Tarazaga. Modal parameter uncertainty estimates as a tool for automated operational modal analysis: Applications to a smart building. In *Dynamics of Civil Structures, Volume 2*, pages 177–182. Springer, 2019.

[64] Javier Schloemann, V.V.N. Sriram Malladi, Americo G. Woolard, Joseph M. Hamilton, R. Michael Buehrer, and Pablo A. Tarazaga. Vibration event localization in an instrumented building. In *Experimental Techniques, Rotating Machinery, and Acoustics, Volume 8*, pages 265–271. Springer, 2015.

[65] Michael Schwenk, Carol Howe, Ahlam Saleh, Jane Mohler, Gurtej Grewal, David Armstrong, and Bijan Najafi. Frailty and technology: A systematic review of gait analysis in those with frailty. *Gerontology*, 60(1):79–89, 2014. ISSN 1423-0003, 0304-324X. doi: 10.1159/000354211.

[66] Michael Schwenk, Jane Mohler, Christopher Wendel, Mindy Fain, Ruth Taylor-Piliae, Bijan Najafi, et al. Wearable sensor-based in-home assessment of gait, balance, and physical activity for discrimination of frailty status: Baseline results of the arizona frailty cohort study. *Gerontology*, 61(3):258–267, 2015.

[67] Tim Sharpe. Ethical issues in domestic building performance evaluation studies. *Building Research & Information*, 47(3):318–329, 2019.

[68] Shelley A. Sternberg, Andrea Wershof Schwartz, Sathya Karunananthan, Howard Bergman, and A. Mark Clarfield. The identification of frailty: A systematic literature review. *Journal of the American Geriatrics Society*, 59(11):2129–2138, Nov 2011. ISSN 00028614. doi: 10.1111/j.1532-5415.2011.03597.x.

[69] Shelley A. Sternberg, Andrea Wershof Schwartz, Sathya Karunananthan, Howard Bergman, and A. Mark Clarfield. The identification of frailty: A systematic literature review. *Journal of the American Geriatrics Society*, 59(11):2129–2138, Nov 2011. ISSN 00028614. doi: 10.1111/j.1532-5415.2011.03597.x.

[70] Erik E. Stone and Marjorie Skubic. Passive in-home measurement of stride-to-stride gait variability comparing vision and kinect sensing. In *2011 Annual International Conference of the IEEE Engineering in Medicine and Biology Society*, pages 6491–6494. IEEE, 2011.

[71] Stephanie Studenski, Risa P. Hayes, Ruth Q. Leibowitz, Rita Bode, Laurie Lavery, Jeremy Walston, Pamela Duncan, and Subashan Perera. Clinical global impression of change in physical frailty: Development of a measure based on clinical judgment. *Journal of the American Geriatrics Society*, 52(9):1560–1566, 2004. doi: https://doi.org/10.1111/j.1532-5415.2004.52423.x. URL https://agsjournals.onlinelibrary.wiley.com/doi/abs/10.1111/j.1532-5415.2004.52423.x.

[72] Adane Tarekegn, Fulvio Ricceri, Giuseppe Costa, Elisa Ferracin, and Mario Giacobini. Detection of frailty using genetic programming. In Ting Hu, Nuno Lourenço, Eric Medvet, and Federico Divina, editors, *Genetic Programming*, pages 228–243. Springer International Publishing, 2020.

[73] Adane Tarekegn, Fulvio Ricceri, Giuseppe Costa, Elisa Ferracin, and Mario Giacobini. Predictive Modeling for Frailty Conditions in Elderly People: Machine Learning Approaches. *JMIR Med Inform*, 8(6):e16678, Jun 2020. ISSN 2291-9694. doi: 10.2196/16678. URL http://medinform.jmir.org/2020/6/e16678/.

[74] Can Tunca, Nezihe Pehlivan, Nağme Ak, Bert Arnrich, Gülüstü Salur, and Cem Ersoy. Inertial sensor-based robust gait analysis in non-hospital settings for neurological disorders. *Sensors*, 17(4):825, 2017.

[75] Nicola Veronese, Brendon Stubbs, Stefano Volpato, Giovanni Zuliani, Stefania Maggi, Matteo Cesari, Darren M. Lipnicki, Lee Smith, Patricia Schofield, Joseph Firth, Davy Vancampfort, Ai Koyanagi, Alberto Pilotto, and Emanuele Cereda. Association between gait speed with mortality, cardiovascular disease and cancer: A systematic review and meta-analysis of prospective cohort studies. *Journal of the American Medical Directors Association*, 19(11):981–988.e7, 2018. ISSN 1525-8610. doi: https://doi.org/10.1016/j.jamda.2018.06.007. URL https://www.sciencedirect.com/science/article/pii/S152586101830327X.

[76] Federico Viani, Mauro Martinelli, Luca Ioriatti, Manuel Benedetti, and Andrea Massa. Passive real-time localization through wireless sensor networks. In *2009 IEEE International Geoscience and Remote Sensing Symposium*, volume 2, pages II–718. IEEE, 2009.

[77] Tyler Williamson, Sylvia Aponte-Hao, Bria Mele, Brendan C. Lethebe, Charles Leduc,

Manpreet Thandi, Alan Katz, and Sabrina T. Wong. Developing and validating a primary care emr-based frailty definition using machine learning. *International Journal of Population Data Science*, 5, Sep 2020. ISSN 2399-4908. doi: 10.23889/ijpds.v5i1.1344. URL https://ijpds.org/article/view/1344.

[78] Americo G. Woolard and Pablo A. Tarazaga. Applications of dispersion compensation for indoor vibration event localization. *Journal of Vibration and Control*, 24(21): 5108–5117, 2018. doi: 10.1177/1077546317744997. URL https://doi.org/10.1177/1077546317744997.

[79] Damiano D. Zemp, Olivier Giannini, Pierluigi Quadri, and Eling D. de Bruin. Gait characteristics of ckd patients: a systematic review. *BMC Nephrology*, 20(1):1–12, 2019.

[80] J.A. Zeni Jr., J.G. Richards, and J.S. Higginson. Two simple methods for determining gait events during treadmill and overground walking using kinematic data. *Gait & Posture*, 27(4):710–714, 2008.

[81] José A. Ávila Funes, Hélène Amieva, Pascale Barberger-Gateau, Mélanie Le Goff, Nadine Raoux, Karen Ritchie, Isabelle Carrière, Béatrice Tavernier, Christophe Tzourio, Luis Miguel Gutiérrez-Robledo, and et al. Cognitive impairment improves the predictive validity of the phenotype of frailty for adverse health outcomes: The three-city. *Journal of the American Geriatrics Society*, 57(3):453–461, Mar 2009. ISSN 00028614, 15325415. doi: 10.1111/j.1532-5415.2008.02136.x.